

# Spacecraft Structures and Launch Vehicles

Lyonel Abou Nassar

Robert Bonifant

Cody Diggs

Eric Hess

Robert Homb

Lauren McNair

Eric Moore

Philip Obrist

Mike Southward

November 18, 2004

# Contents

<b>List of Figures</b>	<b>iv</b>
<b>Abbreviations</b>	<b>v</b>
<b>Symbols</b>	<b>vi</b>
<b>1 Introduction</b>	<b>1</b>
1.1 Launch Vehicles . . . . .	1
1.1.1 Launch Vehicles Available . . . . .	1
1.1.2 Launch Vehicle Capabilities . . . . .	2
1.1.3 Deciding which Launch Vehicle to Use . . . . .	2
1.1.4 Characteristics of Spacecraft Necessary to Choose a Launch Vehicle . . . . .	2
1.2 Structures . . . . .	3
1.2.1 Primary Structural Design . . . . .	3
1.2.2 Other Functional Divisions . . . . .	3
1.2.3 Mechanisms Used by the Other Subsystems . . . . .	5
1.2.4 Materials for Constructing Spacecraft . . . . .	5
1.2.5 Manufacturing Techniques Applicable to the Structure . . . . .	7
1.3 Summary . . . . .	8
<b>2 Modelling and Analysis</b>	<b>9</b>
2.1 Structures . . . . .	9
2.1.1 Loads and Stresses . . . . .	9
2.1.2 Thin-Walled Pressure Vessels . . . . .	13
2.1.3 Buckling of Beams . . . . .	15
2.1.4 Thin-Wall Assumption . . . . .	17
2.1.5 Finite Element Analysis . . . . .	18
2.2 Materials . . . . .	23
2.3 Vibrations . . . . .	31
2.3.1 Flexible Body Dynamics . . . . .	32
2.3.2 Orbital Vibration Mitigation . . . . .	33
2.3.3 Vibrations Summary . . . . .	34

2.4	Launch Vehicle Connector . . . . .	34
2.4.1	Launch Vehicle Theory . . . . .	35
2.4.2	Expanding the CMM . . . . .	36
2.4.3	Launch Vehicle Summary . . . . .	38
2.5	Summary . . . . .	38
<b>3</b>	<b>Technologies and Examples</b>	<b>39</b>
3.1	Available Technologies . . . . .	39
3.1.1	Available Launch Vehicles . . . . .	39
3.1.2	Beams . . . . .	44
3.1.3	Spacecraft Mechanisms . . . . .	45
3.2	New Technologies . . . . .	49
3.2.1	Inflatable Structures . . . . .	49
3.2.2	Magnetically Inflated Cable System . . . . .	51
3.2.3	Flying Effector . . . . .	53
3.2.4	Nanotubing . . . . .	54
3.3	Examples . . . . .	56
3.3.1	Load and Deflection Nodal Analysis Example . . . . .	56
3.3.2	Material Selection Analysis Example . . . . .	58
3.3.3	Self Strained Example . . . . .	58
3.3.4	Reaction Wheel Example . . . . .	63
3.3.5	Space Shuttle Landing Example . . . . .	64
3.3.6	Vibrations Example . . . . .	66
3.4	Conclusion . . . . .	68
<b>4</b>	<b>Conclusions</b>	<b>69</b>
4.1	Structures . . . . .	69
4.2	Vibrations . . . . .	70
4.3	Materials . . . . .	71
4.4	Launch Vehicles . . . . .	72
4.5	New Technologies . . . . .	75
4.6	Summary . . . . .	76
	<b>Bibliography</b>	<b>77</b>

# List of Figures

2.1	Normal Stress <sup>1</sup> . . . . .	10
2.2	Shear Stress <sup>1</sup> . . . . .	10
2.3	Bearing Stress <sup>1</sup> . . . . .	11
2.4	Hoop Stress Element <sup>1</sup> . . . . .	14
2.5	Longitudinal Stress Element <sup>1</sup> . . . . .	15
2.6	Radial Stress Element <sup>1</sup> . . . . .	15
2.7	Cross-Section of Beam <sup>19</sup> . . . . .	17
2.8	Simple 2-D FEA element. . . . .	18
2.9	Free Body Diagram of the Bar and Its End Nodes. <sup>19</sup> . . . . .	21
2.10	Magnetic Field and Magnetic Flux in a Coil <sup>5</sup> . . . . .	26
2.11	Spectrum of Electromagnetic Waves <sup>5</sup> . . . . .	27
2.12	Strength as a Function of Density <sup>5</sup> . . . . .	28
2.13	Stress-Strain Graph . . . . .	29
2.14	Isotropic Positive Poisson's Ratio . . . . .	29
2.15	The geometry of surface and internal crack <sup>5</sup> . . . . .	30
2.16	Frequency Ranges for Shock and Vibration Attenuation Systems <sup>18</sup> . . . . .	31
2.17	Reusable magnetic isolation system <sup>10</sup> . . . . .	34
2.18	Description of Rocket DOF <sup>20</sup> . . . . .	36
3.1	Table of Launch Vehicle Data <sup>15</sup> . . . . .	40
3.2	Diagram of Qwknut Mechanism <sup>7</sup> . . . . .	47
3.3	Diagram of Solar Panels Mechanisms <sup>12</sup> . . . . .	48
3.4	Picture of Modules Built By Bigelow Aerospace <sup>9</sup> . . . . .	50
3.5	ARISE Looking Into Deep Space <sup>6</sup> . . . . .	52
3.6	Initial Solution to Large Space Construction <sup>2</sup> . . . . .	53
3.7	More Efficient Solution to Large Space Structure Construction. <sup>2</sup> . . . . .	54
3.8	Application of Effector Use <sup>2</sup> . . . . .	54
3.9	Nanotubing <sup>8</sup> . . . . .	55
3.10	Nanotubing Sheet <sup>8</sup> . . . . .	55
3.11	Five-bar truss example <sup>20</sup> . . . . .	57
3.12	Heated structure <sup>20</sup> . . . . .	59
3.13	FBD of the heated structure <sup>20</sup> . . . . .	59
3.14	FBD of the heated structure <sup>20</sup> . . . . .	62

3.15 Setup diagram for the wheel and the motor <sup>13</sup> . . . . .	64
3.16 Simplified landing gear <sup>13</sup> . . . . .	65

## Abbreviations

ACS	Assembly & Command Ship
ARISE	Advanced Radio Interferometry between Space and Earth
AFB	Air Force Base
AFS	Air Force Station
CC&DH	Communications, Command, & Data Handling
CFRP	Carbon Fiber Reinforced Polymers
CMM	Consistent Mass Matrix
D&C	Dynamics & Controls
DOF	Degrees of Freedom
DPS	Defense Program Support
EGI	Embedded GPS/INS
ESA	European Space Agency
FEA	Finite Element Analysis
FBD	Free-Body Diagram
GEO	Geo-stationary Orbit
GPS	Global Positioning System
GTO	Geosynchronous Transfer Orbit
HTS	High Temperature SC
INS	Inertial Navigation System
ISS	International Space Station
LEO	Low Earth Orbit
LOX	Liquid Oxygen
LTS	Low Temperature SC
LV	Launch Vehicles
LVA	Launch Vehicle Adapter
ODE	Ordinary Differential Equation
MIC	Magnetically Inflated Cable
MLI	Multi-Layer Insulation
NASA	National Aeronautic & Space Administration
OCA	Orbital Carrier Aircraft
PT&E	Power, Thermal, & Environment
RRDI	Restraint, Release, and Deployment-Initiation
S&LV	Structures & Launch Vehicles
SC	Super-Conducting
SADM	Spring Activated Deployment Mechanisms
SMAD	Space Mission Analysis & Design
SUITE	Satellite Ultraquiet Isolation Technology Experiment
TWDM	Torsional Wheel Deployment Mechanism
VBLI	Very Large Baseline Interferometry

# Symbols

$\alpha_l$	Linear Coefficient of Thermal Expansion
$B$	Magnetic Field Strength
$C$	Energy Required to Produce a Unit Temperature Rise
$\varepsilon$	Strain
$\varepsilon_x$	Axial Strain
$\varepsilon_y$	Lateral Strain
$\varepsilon_z$	Lateral Strain
$E$	Young's Modulus
$\{F\}$	Force Matrix
$\{F_g\}$	Modal Force Matrix
$F.S.$	Factor of Safety
$G$	Shear Modulus
$H$	Externally Applied Magnetic Field Strength
$I$	Moment of Inertia
$J$	Polar Moment of Inertia
$k$	Spring Stiffness Constant
$[K]$	Stiffness Matrix
$[K_g]$	Modal Stiffness Matrix
$K_c$	Fracture Toughness
$\frac{l}{k}$	Critical Slenderness Ratio
$M$	Bending Moment
$[M]$	Mass Matrix
$[M_g]$	Modal Mass Matrix
$\mu$	Permeability
$N$	Axial Force
$n_{max}$	Maximum Load Factor LVA Will Undergo
$\vec{Q}$	Nodal Force Vector
$\vec{Q}^0$	Fixed-End Nodal Force Vector
$P$	Pressure Force in a Pressure Vessel
$P_{cr}$	Critical Pressure in a Pressure Vessel
$[\Phi]$	Modal Vector Matrix
$q$	Thermal Conductivity
$\{q\}$	Modal Displacement Vector
$q_i$	Displacement at Each Node
$Q_i$	Forces Acting on Nodes
$\rho$	Resitivity (Materials Section)
$\rho$	Density
$\sigma$	Axial Stress(Structures Section)
$\sigma$	Thermal Stresses Materials Section

$\sigma_b$	Bearing Stress
$\sigma_c$	Critical Stress Required for Crack to Propagate
$\sigma_h$	Internal Force in a Pressure Vessel
$\sigma_l$	Longitudinal Stress in a Pressure Vessel
$\sigma_r$	Radial Stress in a Pressure Vessel
$\sigma_x$	Normal Stress
$\sigma_{max}$	Maximum Allowable Stress
$T$	Torque
$\tau$	Shear Stress
$\tau_t$	Maximum Torsional Stress
$\{u\}$	Nodal Displacement Vector
$\{\ddot{u}\}$	Nodal Acceleration Vector
$\nu$	Poisson's Ratio
$V$	Voltage
$V_1(z)$	Shear Force
$\omega$	Resonant Frequency
$y$	Distance from Center Axis

# Chapter 1

## Introduction

Throughout the structures functional division many areas of concentration are needed, from the selection of launch vehicles to the types of structures used. Without a launch vehicle the payload cannot reach orbit, so the criteria for selecting a launch vehicle must be presented. The structure of the payload is most important during lift-off, when forces are greatest upon the payload and these forces must be studied.

### 1.1 Launch Vehicles

The launch vehicle group has the responsibility of selecting the launch vehicle and designing the interaction between the launch vehicle and the payload to be used in each mission. Each available launch vehicle has different payload characteristics including: the amount of force the payload will endure, the dimensions on the centaur, and where the payload is stored. The choice of a launch vehicle that will put the payload into the proper orbit for the mission is important. Thus, the launch vehicle group needs the size, mass, and orbital destination of the spacecraft to make an educated selection of a launch vehicle.

#### 1.1.1 Launch Vehicles Available

There are many launch vehicles are available for use. This section concentrates on eight specific launch vehicles. The seven launch vehicles described in this section include five American launch vehicles, one European launch vehicle, and one Russian launch vehicle. The American launch vehicles included in this section are the Atlas, K-1, Delta, Pegasus, and Taurus launch vehicles. Also included in this section are: the European launch vehicle the Ariane, and the Russian launch vehicle the Zenit.<sup>15</sup>

### **1.1.2 Launch Vehicle Capabilities**

The design team has to know what the capabilities of the launch vehicles are in order to make an educated decision of which launch vehicle is to be used. Using criteria such as lift capacity, size of the centaur, and the maximum altitude, the team can narrow the options down to a few launch vehicles. Different alternatives are discussed to give an idea of the types of launch vehicles available.

### **1.1.3 Deciding which Launch Vehicle to Use**

Determining which launch vehicle meets the needs of the mission depends on various factors ranging from maximum payload capacity to the forces the vehicle produces on the payload during lift-off. If the mission requires a payload of 500kg, the Pegasus launch vehicle would not be chosen since it can only carry a payload of 450kg. The design team must choose a launch vehicle that has the lift capacity to support the mission. The launch vehicle must also be reliable because the payload is expensive.

Ideally, the design team wants the launch vehicle to create little or no vibrations, however, in reality, engine oscillations and other components of the launch vehicle produce vibrations that need to be accounted. The amount of vibration that the payload endures is dependent on the launch vehicle chosen. Therefore, choosing a launch vehicle that minimizes these vibrations is essential.

The launch vehicle needs to be able to reach the orbit that the mission intends. A launch vehicle aimed at taking payloads to LEO would not be used in a mission that requires a GEO orbit. The inclination of the orbit needs to be considered when selecting the launch vehicle as well. Obtaining a certain inclination angle is dependent on where the launch takes place. A launch vehicle would be chosen that can obtain the inclination angle the mission requires.

### **1.1.4 Characteristics of Spacecraft Necessary to Choose a Launch Vehicle**

The spacecraft needs to work well with a launch vehicle since designing a new launch vehicle would not be the best course of action. Some of the criteria required are the spacecraft's overall dimensions, mass, altitude destination, and attitude destination. The design group must choose a launch vehicle that will fit the payload. Depending on which launch vehicle is selected; there are only certain inclination angles where the vehicle can be launched to, all depending on the launch site. In order to get a payload to a given altitude the vehicle must be powerful enough to reach the necessary orbit. For instance, a Pegasus would not be able to reach GEO. Other characteristics could be considered, but are not as necessary as the ones listed above. The design of the structure of the payload is primarily based on forces incurred during lift-off.

## 1.2 Structures

The structure of the payload holds together the rest of the payload. It prevents the launch vibrations from destroying or harming critical parts of the payload. In the following sections topics such as material selection, spacecraft mechanisms, and manufacturing techniques are discussed.

### 1.2.1 Primary Structural Design

The primary structural design is important to the mission because the mission would not be possible without it. There are several factors that drive the design process; financial limitations, the goals of the mission, and the physical constraints are some of the limitations that the launch vehicle places on the mission. There are many other possible factors that drive the design process that will not be discussed due to the insignificance compared to the previously discussed factors.

Financial limitations is always one of the most important factors in the design process. The financial constraints determine whether the project can use the best materials and technologies available or whether the project will have to settle for inferior equipment. When a spacecraft is launched into orbit a large amount of money is going to be needed, such as billions of dollars to launch a deep space probe, and thus the cost factor is apparent. Within the structural design, budgetary constraints determine whether the project can use titanium or carbon fiber reinforced polymers.

The structural design team is responsible for assembling all the components in a way as to minimize the size of the spacecraft. The structural design cannot be contemplated without knowing what equipment will be used. The other functional groups are responsible for giving the design team the dimensions and properties of the hardware. Once this information is known, then the design of the primary structural members can begin.

The launch vehicle selection is the most important piece of information for the engineering of the spacecraft. During lift-off, the spacecraft experiences the maximum forces due to the high acceleration, vehicle vibrations, and the weight of the spacecraft upon itself. The choice of the launch vehicle will tell the design team the forces that the payload will endure. Usually, the choice of the launch vehicle is made based on the mission parameters and not the other way around. One of these parameters is that the spacecraft must be able to fit inside of the top of the launch vehicle. In order to properly design the payload information from other functional divisions will be needed.

### 1.2.2 Other Functional Divisions

An abundant amount of information is required by all other functional divisions within this project in order to have a successful mission. If this information is not adequately

communicated, the entire project will be at a loss of both time and money. Therefore it is vital to the outcome of the mission that the other functional divisions supply the following information. More information will obviously need to be accumulated as the project progresses.

From Dynamics and Controls, D&C, the most vital information needed is the postulated missions and corresponding orbital types. The information provided by the D&C will enhance the design team's ability to decide on the required structures for all phases of the mission in each orbit, so the outcome will be successful. The required mission and orbital subsystems are needed in order to allow for sizing and selecting appropriate structures for containment and deployment features. The subsystems include but are not limited to: guidance and navigation, maintenance, power, and deployables. The projected propulsion methods also need to be obtained, which will allow the team to adequately select all structures required starting from liftoff to return. The total mass of the D&C system and subsystems is required for further structural analysis.

The Power, Thermal, and Environment functional division, PT&E, also collaborates heavily with the team's functional division. The team needs to know the equipment that will power the mission from start to finish; with this information, the team can develop the appropriate structures required to contain the power systems and subsystems. Knowledge of their selection of insulation, radiators, and other thermal paraphernalia will help S&LV determine imposed structural constraints. All alternatives for controlling power, temperature, and environment as well as all required subsystems for those fields are desired to describe the appropriate structural selection.

Adequate correlation with the Communications, Command and Data Handling, CC&DH, functional division also needs to be instituted. All of their selected receivers, transmitters, and antennas need to be evaluated to select appropriate attachment and deployment structures. At the same time, knowledge of their communication interfaces, architectures, and data bus candidates would be helpful in the design and implementation of appropriate structural needs. After this information is provided, the S&LV team will be able to provide the most fitting solution for the structural requirements.

Payloads, mission operations, and ground systems requirements also need to be analyzed by the S&LV team to sufficiently provide appropriate structures for support and deployment. Also, the ground based teams alternatives are required to justify more optimal solutions. The information received by all the functional divisions needs to be carefully analyzed, so the final structural specifications can be determined and implemented. Strong communication is vital; any lack of communication could prove detrimental to the outcome of the mission.

### 1.2.3 Mechanisms Used by the Other Subsystems

A spacecraft needs mechanisms in order to properly function. In order to keep the spacecraft oriented correctly, it will need momentum wheels and control moment gyros (CMGs). A retractable boom has small moving mechanisms that extend and retract the boom when needed. These mechanisms, and the subsystems that use the mechanisms, are studied in this section.

Aerospace mechanisms can be placed into two categories, high-cyclic and low-cyclic. A high-cyclic mechanism, such as those used in antenna pointing and tracking or boom extensions, requires frequent or constant movement. The low-cyclic mechanisms, however, are used to restrain payloads during launch and retrieval. The most challenging requirements for mechanisms are those that demand precision pointing and a long operating life.<sup>21</sup>

When designing a spacecraft, three key elements to keep in mind are: mass, power, and volume. In most cases, the design would focus on reducing these three elements, but the design of the mechanisms must focus on making the mechanisms operable. Most mechanisms do not require a great deal of power. Low-cyclic mechanisms only operate a few times per mission and high-cyclic mechanisms only draw a large voltage during the acceleration phase of the duty cycle. This acceleration phase normally accounts for 10% of the high-cyclic mechanisms operating life. The volume may have to be constrained to fit in a certain position in the spacecraft, but denser, stronger materials can be used to strengthen the mechanisms.

Each mechanism will have its own requirements for forces, operating rates, structural stiffness, operating life, and environments.<sup>21</sup> The strength and stiffness requirements may depend on the mechanism being able to withstand the launch and derived vibration tests. Another key concern is thermal influences, because the spacecraft will be operating in outer space, where temperatures can rise and fall rapidly. The thermal influence will affect which materials are chosen, as well as lubricants and coatings. The thermal influences will cause different materials to expand at different rates which will cause additional loads on the structures.

### 1.2.4 Materials for Constructing Spacecraft

Material selection plays a large role in constructing a spacecraft. The materials available and the types of structures desired are two of the main factors in choosing the materials for the spacecraft. The methods of construction for the structures play a role in material selection. After options are weighed and decided upon, the materials undergo an assessment based on the weight, cost, and benefits of the material. The important properties of the materials are: strength, stiffness, ductility, density, fracture toughness, thermal conductivity, thermal expansion, corrosion resistance, ease of fabrication, versatility, availability, and cost. Materials are important to all aspects of the spacecraft including dynamics and control, power, and the overall mission. After the materials are determined and analyzed, the materials that fit the space-

craft's requirements and maximize performance are selected for the construction of the spacecraft.<sup>3,16</sup>

The primary materials used for spacecraft applications are: aluminum and aluminum alloys, steel and heat-resistant steel, magnesium, beryllium, titanium, and composites. All of these materials have desirable and undesirable qualities. For example, aluminum is easy to machine and has a high strength per weight ratio, but it has a high coefficient of thermal expansion and a low hardness; however, aluminum is a preferable material for the main structure of the spacecraft because the mass of the spacecraft is one the primary concerns when designin the spacecraft. Steel is not a desirable material in the construction of the spacecraft because of the mass constraint. In addition, steel is magnetic and hard to machine. Magnesium is a commonly used spacecraft material, because it has a low density, but it is susceptible to corrosion and it has a low yield strength. Titanium has a high strength and low weight, but it is hard to machine (costly) and it has low fracture toughness. Beryllium has a high stiffness per density ratio, but it also has a low ductility and fracture toughness. Finally, composites are preferable because of their low density and strength in tension, but are insufficient in compression, brittle, and costly. All of these factors take part in the selection of the materials for the final spacecraft design.<sup>3,16</sup>

Many considerations go into the selection of materials for the construction of a spacecraft. Some of the main considerations are flammability, toxicity, off-gassing and out-gassing, stress corrosion cracking, and contamination. The structure must be able to survive the trip to its destination and the environment of space that it is placed in. The dynamics and control and the efficiency of the spacecraft are directly related to the materials used to construct the spacecraft. The payload will also influence the materials chosen for the spacecraft. The payload is the most important part of the spacecraft, and the materials of the spacecraft should not interfere with the function of the payload. The communications and computer systems of the spacecraft should also not be negatively affected by the materials of the spacecraft. The material's thermal conductivity, corrosion resistance, and other traits can have an effect on the functionality of these systems. The power system of the spacecraft should maximize the power and minimize the weight of the spacecraft without interfering with the function of the other systems on the spacecraft. The dynamics and control, computer and communication systems, power system, and payload need to be taken into consideration when selecting materials for the construction of the spacecraft.<sup>3,16</sup>

The selection of materials for the design of a spacecraft is critical for its survival, efficiency, and function. The selection process will begin with a list of the available materials; then, the list will be narrowed down by analyzing the properties of the materials.

### 1.2.5 Manufacturing Techniques Applicable to the Structure

Hardware manufacture is an important part of the design process, because it influences the cost and schedule of the project. The classification of hardware types includes: piece parts, components, assembly, subsystems and the spacecraft. The assembly type involves parts such as: a hinge assembly, an antenna feed or a deployment boom. Methods of manufacturing spacecraft are derived from the electronics and aircraft industries. The main difference from the aircraft industry is the difficulty to service a spacecraft in orbit, thus spacecraft recalls are almost non-existent. In addition, the biggest stress experienced by the spacecraft is during the launch, while for an airplane the biggest stress is during a bank of the airplane.<sup>21</sup>

In order to start the manufacturing process, complete schematics and material selection information are needed. The manufacturing process can be broken into four subcategories. Manufacture planning, which typically is done at the same time as the engineering data preparation, consists of translating the engineering data into manufacturing plans, aids, and tooling. The process of the manufacture planning continues with preparing detailed procedures for assembling the parts and examining the different inspections and tests that are required. An analysis of the facilities needed for these assembly and test procedures, as well as the manufacturing methods must be done. In order to ensure no injuries occur during the manufacturing process, precautions have to be taken, including the training and certifications levels of personnel. Manufacturing facilities, include mechanical manufacturing, electronic manufacturing, spacecraft assembly and testing. Mechanical manufacturing covers a wide range of processes such as plating and chemical treatment, elevated temperature treatment, adhesive bonding, and composite manufacturing.<sup>21</sup>

Spacecraft assembly and test operations are performed in a controlled-cleanliness environment usually. The testing of the spacecraft requires large vibration and vacuum equipment. After the plans have been well established, the manufacturing process can be written with all the required details. This detailed process travels with the hardware as a checklist and becomes part of the permanent record of the manufacturing process. The next section is parts procurement and testing, which can take up to eighteen months and is the longest process, as the parts required often have to undergo a series of expensive and time consuming testing. All components are negotiated for their price, which may add a few months to the procurement time. Component assembly, which typically takes about one to three months, requires different facilities with different level of cleanliness depending on the part assembled, it can range from a class 100 to not controlled at all. Some of the payload parts may require cryogenic temperature absence of magnetic fields, which requires special and expensive facilities. Component acceptance that includes functional testing and environmental exposure takes one to three months.<sup>21</sup>

## 1.3 Summary

There are many constraints and criteria that need to be known before deciding the right structure and launch vehicle. Major constraints needed to be fulfilled include orbit elevation, eccentricity, and other orbit parameters. These constraints are necessary to choose the right launch vehicle for a given mission from a known launch site. The primary design of the spacecraft is influenced by many factors ranging from the budget to the type of mission that is being launched. Mechanisms are also part of the structural design for a spacecraft. Each component must be engineered specifically for cost, weight, functionality, and size. Materials are also of important consideration because they have to withstand loads during launch while maintaining structural integrity. The materials also must be able to be machined with the manufacturing techniques available. Of all constraints applied to the structure and launch vehicle, the budget must be maintained or else the mission will be terminated.

# Chapter 2

## Modelling and Analysis

The design of a spacecraft requires careful examination of the structural components. The structure must be designed to handle the loads that cause stresses, strains, bending, shearing, and other structural demands. The launching of the payload causes vibrations, which in turn creates loads on the structure. These vibrations are complex, but must be modeled in order to determine the loads that act on the payload. The materials are mainly chosen based on the loads caused during lift-off and re-entry as well as stresses created by orbital maneuvers. Other properties of the materials could be important depending on their uses. An analysis of the loads that the spacecraft will endure during its lifetime allows materials with the appropriate attributes to be selected.

### 2.1 Structures

The structure of a spacecraft is designed to maintain shape and structural integrity against axial loading, strain, torsion, shearing, and buckling. Spacecraft design requires analysis of these stresses; but, when analyzing the entire structure of a spacecraft, the analysis can become rigorous and complicated. When the structure becomes complicated, certain assumptions can be made to simplify structural equations to analyze each critical section. More complicated structural analysis requires other approaches that require the use of a computer to solve complicated equations.

#### 2.1.1 Loads and Stresses

The main objective of the study of the mechanics of materials is to provide the future engineer with the means of analyzing and designing various machines and load-bearing structures.<sup>4</sup> The means of analyzing and designing various machines and load-bearing structures can be accomplished by understanding the various forces that are applied to structures, and the strains created by the stresses. The term stress is defined as the magnitude of a force distributed over a given area. The stress depends on the

applied forces or torques, and occurs as an axial, shearing, or bearing load. Axial stress,  $\sigma$ , is developed in a cross-sectional area,  $A$ , when it is subjected to a normal Force  $F$ , and is given by:

$$\sigma = \frac{F}{A} \quad (2.1)$$

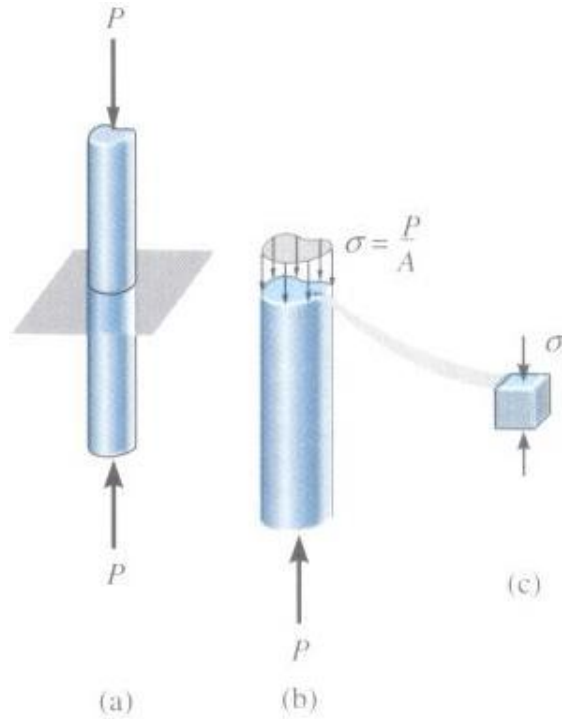


Figure 2.1: Normal Stress<sup>1</sup>

A compressive force causes a compressive stress, and a tensile force causes a tensile stress.

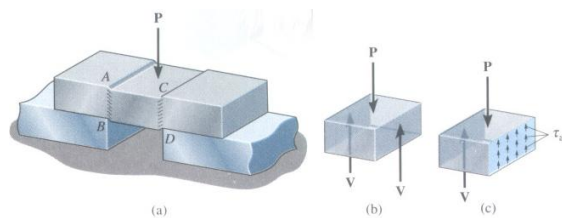


Figure 2.2: Shear Stress<sup>1</sup>

Shearing stress,  $\tau$ , occurs when transverse loads are applied to the cross-section of a member. These forces,  $P$ , are perpendicular to the axial forces and are applied

to the same cross-sectional area,  $A$ . The relationship is given by:

$$\tau = \frac{P}{A} \quad (2.2)$$

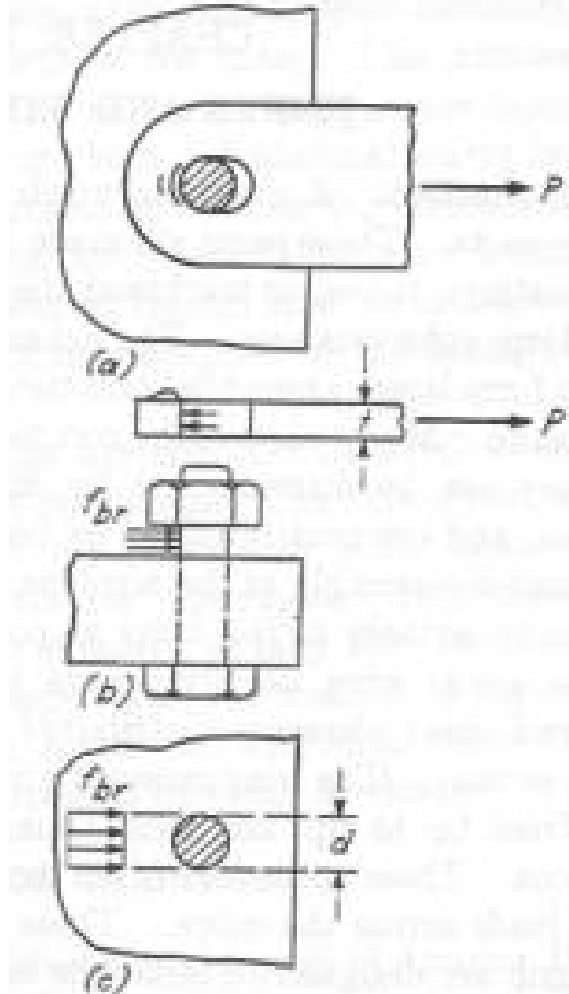


Figure 2.3: Bearing Stress<sup>1</sup>

Bearing stress occurs at areas where bolts, pins, and rivets create stress in the members to which they are connected. This kind of stress occurs along the bearing surface, or the surface of contact. An average nominal value is typically used because the distribution of these stresses is quite complicated. This value represents the bearing stress,  $\sigma_b$ , where the load,  $P$ , is divided by the area of the rectangle,  $t \times d$ , that represents the projection of the bolt on the plate, which is given by:

$$\sigma_b = \frac{P}{td} \quad (2.3)$$

When any of these three stresses are present, the structure experiences some level of strain. This strain,  $\varepsilon$ , is defined as the deformation of the member,  $\Delta L$ , per unit length,  $L$ , and is given by:

$$\varepsilon = \frac{\Delta L}{L} \quad (2.4)$$

Strain is related to stress through Hooke's Law:

$$\sigma = E\varepsilon \quad (2.5)$$

Equation 2.5 represents the stress with  $\sigma$  and the strain with  $\varepsilon$ . The symbol  $E$  denotes the Modulus of Elasticity, or Young's Modulus, and is a material property that represents the stiffness of the material. Another material property that is frequently used is Poisson's ratio. Poisson's ratio,  $\nu$ , relating the lateral strain,  $\varepsilon_y$ , to the axial strain,  $\varepsilon_x$ , is given by:

$$\nu = -\frac{\varepsilon_y}{\varepsilon_x} \quad (2.6)$$

If Poisson's ratio is known for the material, the lateral strain can be determined from the axial stress and strain. The strain on a structure can also be affected by multi-axial stress, or stress a structure experiences from multiple directions. Multi-axial stresses is often the case with pressure forces, and the strain relationships are given by:

$$\varepsilon_x = \frac{\sigma_x}{E} - \frac{\nu\sigma_y}{E} - \frac{\nu\sigma_z}{E} \quad (2.7)$$

$$\varepsilon_y = \frac{\sigma_y}{E} - \frac{\nu\sigma_x}{E} - \frac{\nu\sigma_z}{E} \quad (2.8)$$

$$\varepsilon_z = \frac{\sigma_z}{E} - \frac{\nu\sigma_x}{E} - \frac{\nu\sigma_y}{E} \quad (2.9)$$

The stresses,  $\sigma$ , and strains,  $\varepsilon$ , experienced are noted by a subscript of the direction in which they are experienced.

The loads a structure experiences are not always forces directed along the axis of a member. The loads can cause torsional and bending effects as well. These effects are caused from torques or moments around a member's axis. Torsional effects are common effects that occur in machines. They tend to occur in shafts where torque is used to drive a motor or mechanical device. The maximum torsional stress,  $\tau_t$ , developed on a cylindrical shaft is given by:

$$\tau_t = \frac{Tc}{J} \quad (2.10)$$

Equation 2.10 shows the maximum torsional stress,  $\tau_t$ , where  $T$  represents the torque,  $c$  represents the distance from the center of the shaft; and  $J$  represents the polar

moment of inertia. The equation for the polar moment of inertia for a cylindrical shaft is given by:

$$J = \frac{1}{2}\pi(r_2^4 - r_1^4) \quad (2.11)$$

Here,  $r_2$  represents the outer radius and  $r_1$  represents the inner radius. These two equations are useful in determining the amount of stress a cylindrical shaft experiences at a particular distance,  $c$ , from the center.

Another effect that loads can create is bending. This effect occurs when a moment is applied to a beam, which causes a tensile stress on one side of the neutral plane and a compressive stress on the opposite side of the neutral plane. The neutral plane is therefore defined as the plane that experiences no stress. The normal stress,  $\sigma_x$ , that the beam experiences is related to the distance from the center axis,  $y$ , which is given by:

$$\sigma_x = -\frac{My}{I} \quad (2.12)$$

Equation 2.12 represents the moment with  $M$  and the area moment of inertia with  $I$ . The area moment of inertia, for a rectangular beam, is given by:

$$I = \frac{1}{12}bh^3 \quad (2.13)$$

Equation 2.13 represents the width with  $b$  and the height with  $h$ . For these equations, the stress experienced is considered to be compressive if  $\sigma_x$  is negative.  $\sigma_x$  is negative when  $y$  is located above the center axis,  $y > 0$ , where the bending moment is positive. The stress is positive when the bending moment is negative.

The effects each stress has on mechanical structure, a factor of safety, F.S., is developed. This term compares the stress, which the structure is being designed to withstand,  $\sigma_e$ , to the ultimate stress,  $\sigma_u$ , this structure can experience before failure. The factor of safety is given by:

$$F.S. = \frac{\sigma_u}{\sigma_e} \quad (2.14)$$

The factor of safety plays an important role when designing any structure. Designing to a factor of safety of one would mean that the structure could operate at the design conditions and be just on the edge of failure. For this reason, the factor of safety is set higher than one so that the structure can operate safely at the design conditions as well as making it unlikely to fail at unusual conditions that were not accounted for.

## 2.1.2 Thin-Walled Pressure Vessels

Thin-walled pressure vessels provide an important application of the analysis of plane stress. In most instances, no bending moment is placed on the vessel walls. So it can

be assumed that the internal forces exerted on the walls are always tangent to the surface of the vessel. The resulting stresses along the wall will be in a plane tangent to the surface of the vessel.

There are two main types of pressure vessels: spherical and cylindrical. A cylindrical vessel is any structure that has a length, constant open cross sectional area and a wall thickness. If we consider a cylindrical vessel of inner radius  $r$  and wall thickness  $t$  containing a fluid placing pressure on the inner surface, plane stresses along the walls can be simplified axial stress along the length of the vessel,  $\sigma_l$ , and axial stress normal to  $\sigma_l$ , called the hoop stress,  $\sigma_h$ . These stresses are a product of the vessels symmetrical axis.

To determine the hoop stress  $\sigma_h$ , the vessel is split in half along a plane that passes through the cylindrical axis as shown in Figure 2.4. In this figure,  $\Delta x$  is the length of a section of the vessel and  $P$  is the internal gauge pressure inside the vessel. Forces perpendicular to the plane cut are defined as  $F_{stress} = \sigma A$  or  $F_{pressure} = PA$ . The resulting forces acting perpendicular to the cut section are: internal force  $\sigma_h = 2t\Delta x$  and pressure force  $P = 2r\Delta x$ . These forces can then be placed in an equilibrium equation perpendicular to the cut plane. The equation for the hoop stress  $\sigma_h$  is then given by:

$$\sigma_h = \frac{pr}{t} \tag{2.15}$$

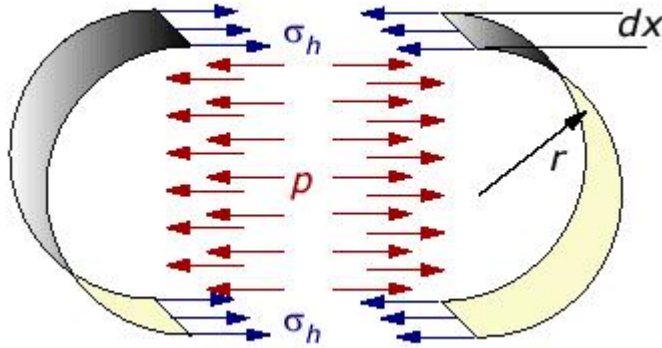


Figure 2.4: Hoop Stress Element<sup>1</sup>

To determine the longitudinal stress  $\sigma_l$ , we make a plane cut perpendicular to the cylindrical axis and consider the forces along that cut section shown in Figure 2.5. Forces acting on the cut section are the internal forces  $\sigma_l \cdot 2\pi r t$  and the pressure force  $P \cdot \pi r^2$ . When the equilibrium solution is solved, the internal stress is given by:

$$\sigma_l = \frac{pr}{2t} \tag{2.16}$$

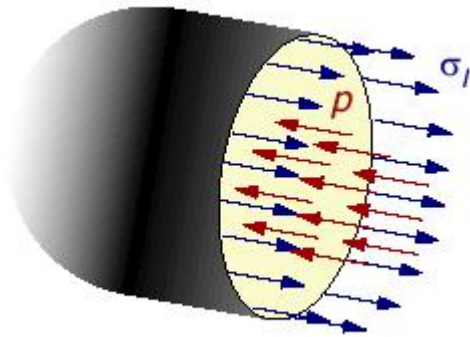


Figure 2.5: Longitudinal Stress Element<sup>1</sup>

Consider a spherical vessel of inner radius  $r$  and wall thickness  $t$ , containing a fluid under gage pressure  $P$ . The stresses on the surface of the wall are equal because of the the vessels symmetry about its center. Internal stress in the wall is called radial stress  $\sigma_r$ . In order to find the radial stress, a plane cut can be made along the center of the vessel, which can be seen in Figure 2.6. This cut section shows the same applied forces that act on the longitudinal section of the cylindrical vessel. The equilibrium solution can then be solved for the radial stress, which is given by:

$$\sigma_r = \frac{Pr}{2t} \quad (2.17)$$

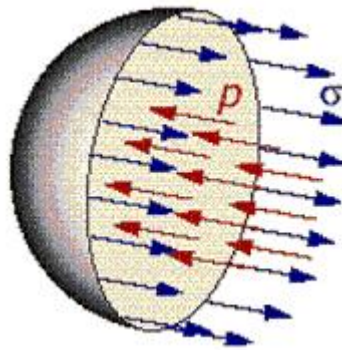


Figure 2.6: Radial Stress Element<sup>1</sup>

### 2.1.3 Buckling of Beams

Buckling is defined as the inability for a structure, normally a beam, to support specified axial loads without undergoing unacceptable deformations. Analysis with

buckling is used most often to choose a column or beam that will fit the constraint imposed and still support the compressive load applied. Compressive members are often defined by their length and according to whether the loading is central or eccentric. There are multiple types of failure do to compressive loading.

The first important term that defines the critical load for a column is the slender ratio ( $l/k$ ), where  $l$  is the length of the column and  $k$  is the radius of gyration of the column. Geometry of the beam defines the radius of gyration and comes from the relationship  $I = Ak^2$ , where  $A$  is the cross sectional area and  $I$  is the moment of inertia.

There are three conditions for which the slenderness ratio defines a different form of failure for a column. The first is the short and stubby beam, which is a column that has material failure before buckling. The critical load,  $P_{cr}$ , that can be placed on this type of beam is given by:

$$P_{cr} = s_y A \quad (2.18)$$

where  $s_y$  is the yield strength of the material. Column material failure will happen while the slenderness ratio ( $l/k$ ) is less than ten. A column with a slenderness ratio greater than or equal to ten will buckle before there is material failure.

The two other types of columns can buckle under a load: intermediate and long-slender. We define the type by comparing the beam slender ratio to a specified critical slenderness ratio  $(l/k)_1$ , given by:

$$\left(\frac{l}{k}\right)_1 = \frac{2\pi^2 CE}{(s_y)^{\frac{1}{2}}} \quad (2.19)$$

where  $C$  is defined as the end condition constant with values shown in Table 2.1 and  $E$  is the modulus of elasticity of the material. When  $(l/k)$  is greater than  $(l/k)_1$ , we define the column to be long and slender. The critical load  $P_{cr}$  is given by:

$$P_{cr} = \frac{C\pi^2 E}{(l/k)^2} \quad (2.20)$$

Equation 2.20 is the Euler equation should be applied to get the critical stress. When the slenderness ratio is less than the the critical slenderness ratio, the column is defined as intermediate. The critical load, defined as the Euler-Johnson equation, is given by:

$$P_{cr} = A \left( s_y - \left( \frac{s_y l}{2\pi k} \right)^2 \frac{1}{CE} \right) \quad (2.21)$$

should be applied to get the critical stress for an intermediate column.

In many instances deviations from an ideal column, such as load eccentricities or crookedness, are likely to occur and thus bending acts on the column and buckling is likely to happen with lesser loads. In this case, the critical load is given by:

Table 2.1: End Condition Constant

Column End Conditions	Theoretical Value	Conservative Value	Recommended Value
Fixed-free	0.25	0.25	0.25
Rounded-rounded	1	1	1
Fixed-rounded	2	1	1.2
Fixed-fixed	4	1	1.2

$$P_{cr} = A s_y \left[ 1 + \frac{ec}{k^2} \sec \left( \frac{l}{2k} \sqrt{\frac{P}{AE}} \right) \right] \quad (2.22)$$

where  $e$  is the eccentricity and  $c$  is the distance from the neutral load on the beam, from bending, to the maximum load along its cross-section.

### 2.1.4 Thin-Wall Assumption

The Thin-Wall Assumption merely helps simplify the equations used in solving a structural problems. We use this assumption because the majority of aerospace structures carry critical loads on thin walled components. The Thin-Walled Assumption is used whenever part of a structural equation places more emphasis on thickness than length; and the length is significantly larger than the thickness. Then that part of the equation can be assumed to be negligible. The following example illustrates the Thin Wall Assumption.<sup>19</sup>

The area moment of inertia of a bar, shown in Figure 2.7, about the X-axis is required to find the shearing load at the base of the bar. This bar is assumed to have a thickness small enough to use the Thin-Walled Assumption.<sup>19</sup>

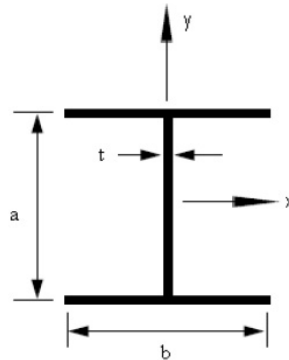


Figure 2.7: Cross-Section of Beam<sup>19</sup>

The area moment of inertia without the Thin-Wall Assumption is given by:

$$I_{xx} = \frac{1}{6}bt^3 + \frac{1}{12}a^3t + 2ba^3t \quad (2.23)$$

Since the thickness is small enough to use the Thin-Wall Assumption, the simplified equation is given by:

$$I_{xx} = \frac{1}{12}a^3t + 2ba^3t \quad (2.24)$$

which shows that the Thin-Wall Assumption can significantly reduce the complexity and size of some structural problems and still produce accurate results. Aerospace Engineers use this technique whenever solving structural problems, but can be simplified with Finite Element Analysis (FEA).<sup>19</sup>

### 2.1.5 Finite Element Analysis

Finite Element Analysis (FEA) for a structure is used to find the deflection, stress, and strain in complex structures that require simultaneous equations to be solved. This method can be used for both statically determinant and indeterminant problems, although statically determinant problems can usually be solved with hand calculations.

The FEA takes a structure and puts it into elements that are connected by nodes. Each element as shown in Figure 2.8 can then be described as a spring with stiffness  $k$  and both end nodes free to move in the direction that the spring stretches. The nodes are labelled  $i$  and  $j$ , where integers  $i \neq j$ . The node forces can be related to the node displacements by the element stiffness matrix, which is given by:

$$\begin{bmatrix} Q_i \\ Q_j \end{bmatrix} = \begin{bmatrix} k_{ii} & k_{ij} \\ k_{ji} & k_{jj} \end{bmatrix} \begin{bmatrix} q_i \\ q_j \end{bmatrix} \quad (2.25)$$

where the forces acting on the nodes are denoted by  $Q$  and displacements at each node are represented by  $q$ .

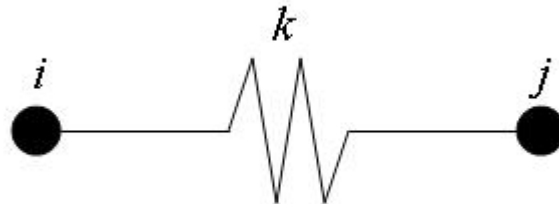


Figure 2.8: Simple 2-D FEA element.

The stiffness matrix,  $[K]$ , can be solved for this simple unrestrained spring given by:

$$[K] = \begin{bmatrix} k & -k \\ -k & k \end{bmatrix} = k \begin{bmatrix} 1 & -1 \\ -1 & 1 \end{bmatrix} \quad (2.26)$$

where the stiffness can be defined using the equation for the deformation of a rod,  $q = QL/(AE)$ . The stiffness  $k$  can then be defined as  $k = AE/L$ . The unrestrained structural stiffness matrix, equation (2.26), has the following properties:

- 1) Matrix  $[K]$  is symmetric; i.e.  $[K]^T = [K]$ .
- 2) The sum of the column elements equals zero.
- 3) The diagonal elements are positive, which must be true on physical grounds.
- 4)  $\det[K] = 0$ ; the matrix is singular because it is unrestrained.

These properties is useful because a beam can be modelled as a spring, and multiple springs can be added together. To further expand this example take two springs,  $a$  and  $b$ , and connect them at one end point. The end nodes for spring  $a$  are labelled  $i$  and  $j$ , and the end nodes for spring  $b$  are labelled  $k$  and  $l$ . A free body diagram will give the following results:

$$q_i = q_1; q_j = q_k = q_2; q_l = q_3 \quad (2.27)$$

$$Q_1 = Q_i; Q_2 = Q_j + Q_k; Q_3 = Q_l \quad (2.28)$$

Inserting equation (2.27) and (2.28) into equation (2.25), the following result is obtained:

$$\begin{bmatrix} Q_1 \\ Q_2 \\ Q_3 \end{bmatrix} = \begin{bmatrix} k_a & -k_a & 0 \\ -k_a & (k_a + k_b) & -k_b \\ 0 & -k_b & k_b \end{bmatrix} \begin{bmatrix} q_1 \\ q_2 \\ q_3 \end{bmatrix} \quad (2.29)$$

This result can be repeated for multiple springs attached together, which allows complex structures, such as a launch vehicle, to be modelled.

Only the force or displacement at a node can be prescribed, but not both. If the node is displaced one millimeter, then the force acting on the node to make that desired displacement can be calculated. Taking the two spring example used before,  $a$  and  $b$ , attached at one node with  $q_1$ ,  $Q_2$ , and  $Q_3$  prescribed. The other values  $Q_1$ ,  $q_2$ , and  $q_3$  can be determined using equation (2.29) by rearranging the equation for known and unknown forces and displacements.

$$\begin{bmatrix} Q_2 \\ Q_3 \\ Q_1 \end{bmatrix} = \begin{bmatrix} (k_a + k_b) & -k_b & -k_a \\ -k_b & k_b & 0 \\ -k_a & 0 & k_a \end{bmatrix} \begin{bmatrix} q_2 \\ q_3 \\ q_1 \end{bmatrix} \quad (2.30)$$

The rearranged stiffness matrix is

$$[K] = \begin{bmatrix} (k_a + k_b) & -k_b & -k_a \\ -k_b & k_b & 0 \\ -k_a & 0 & k_a \end{bmatrix} \quad (2.31)$$

To simplify the math, the following syntax is used

$$\vec{q}_\alpha = \begin{bmatrix} q_2 \\ q_3 \end{bmatrix}; \vec{q}_\beta = [q_1]; \vec{Q}_\alpha = \begin{bmatrix} Q_2 \\ Q_3 \end{bmatrix}; \vec{Q}_\beta = [Q_1] \quad (2.32)$$

$$[K] = \begin{bmatrix} [K_{\alpha\alpha}] & [K_{\alpha\beta}] \\ [K_{\beta\alpha}] & [K_{\beta\beta}] \end{bmatrix} \quad (2.33)$$

where, from equation (2.31), the stiffness matrix can be written as

$$[K_{\alpha\alpha}] = \begin{bmatrix} (k_a + k_b) & -k_b \\ -k_b & k_b \end{bmatrix}; [K_{\alpha\beta}] = \begin{bmatrix} -k_a \\ 0 \end{bmatrix} \quad (2.34)$$

$$[K_{\beta\alpha}] = [-k_a \quad 0] \quad [K_{\beta\beta}] = [k_a] \quad (2.35)$$

The equation (2.34) is called the restrained structural stiffness matrix. The  $\det[K_{\alpha\alpha}] > 0$  so  $[K_{\alpha\alpha}]$  is not a singular matrix because of the prescribed nodal forces and displacements. The matrix equation for the structure in partitioned form

$$\begin{bmatrix} \vec{Q}_\alpha \\ \vec{Q}_\beta \end{bmatrix} = \begin{bmatrix} [K_{\alpha\alpha}] & [K_{\alpha\beta}] \\ [K_{\beta\alpha}] & [K_{\beta\beta}] \end{bmatrix} \begin{bmatrix} \vec{q}_\alpha \\ \vec{q}_\beta \end{bmatrix} \quad (2.36)$$

where an arrow denotes the symbol as being a vector. Carrying out the multiplication equation (2.36) yields

$$\vec{Q}_\alpha = [K_{\alpha\alpha}]\vec{q}_\alpha + [K_{\alpha\beta}]\vec{q}_\beta \quad (2.37)$$

$$\vec{Q}_\beta = [K_{\beta\alpha}]\vec{q}_\alpha + [K_{\beta\beta}]\vec{q}_\beta \quad (2.38)$$

Since  $\vec{Q}_\alpha$  and  $\vec{q}_\beta$  are known, equation (2.37) can be solved for  $\vec{q}_\alpha$ , which contains the unknown displacements.

$$\vec{q}_\alpha = [K_{\alpha\alpha}]^{-1}\vec{Q}_\alpha + [K_{\alpha\alpha}]^{-1}[K_{\alpha\beta}]\vec{q}_\beta \quad (2.39)$$

The unknown nodal displacements are then

$$\begin{bmatrix} q_2 \\ q_3 \end{bmatrix} = \begin{bmatrix} \frac{1}{k_a} & \frac{1}{k_a} \\ \frac{1}{k_a} & (\frac{1}{k_a} + \frac{1}{k_b}) \end{bmatrix} \begin{bmatrix} Q_2 \\ Q_3 \end{bmatrix} - \begin{bmatrix} -1 \\ -1 \end{bmatrix} [q_1] \quad (2.40)$$

The unknown nodal force can then be solved for by placing the nodal displacements calculated from equation (2.40) into equation (2.38). This method can be expanded to other structural problems such as trusses or the heating of a truss bar. However, a different  $[K]$  matrix must be defined to use in these other cases.

## Planar Trusses

The same method used for springs can be used on set of bars connected to form a truss. Each end node is labeled  $i$  and  $j$ , but now the forces can act in a 2D plane instead of only along the direction that the spring stretches. Therefore, the forces are labeled  $Q_{2i-1}$ ,  $Q_{2i}$ ,  $Q_{2j-1}$ , and  $Q_{2j}$  as seen in Figure 2.9. The displacements are represented equivalently but with a lower case  $q$ .

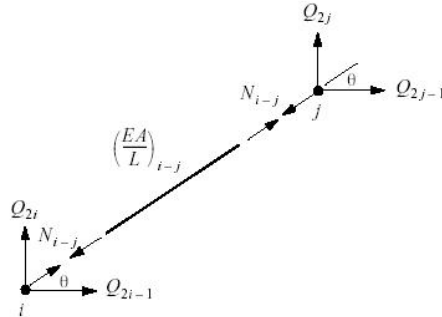


Figure 2.9: Free Body Diagram of the Bar and Its End Nodes.<sup>19</sup>

The unrestrained stiffness matrix for this truss is

$$[ K ] = \frac{EA}{L} \begin{bmatrix} c^2 & cs & -c^2 & -cs \\ cs & s^2 & -cs & -s^2 \\ -c^2 & -cs & c^2 & cs \\ -cs & -s^2 & cs & s^2 \end{bmatrix} \quad (2.41)$$

where  $c$  and  $s$  denote cosine and sine of  $\theta$  shown in Figure 2.9. The unrestrained stress matrix is used to find the unknown displacements and forces on the planar truss. Once the displacements are known, the axial force,  $N$  shown in Figure 2.9, can be determined with

$$N_{i-j} = \frac{EA}{L} [ -c \quad -s \quad c \quad s ] \vec{q}_{i-j} \quad (2.42)$$

The method for solving multiple truss bars is to determine the unrestrained stress matrix for each bar in the truss. The  $[K]$  matrix can then be combined to produce the unrestrained stress matrix of the entire truss.  $[K_{\alpha\alpha}]$  can then be determined and the displacements can be found. Equation (2.42) can then be used to find the axial loads and therefore the stress in each bar.

## Self Strained

A truss bar would be self-strained if it were applied to heat, causing it to expand and apply a force and displacement to the bars to which it is connected. Another form of

self straining is due to lack of fit which could occur if the bar were formed too long or short. The nodal force equation is

$$\vec{Q} = [ K ] \vec{q} + \vec{Q}^0 \quad (2.43)$$

where  $\vec{Q}^0$  is defined as the fixed-end nodal force vector.  $\vec{Q}^0$  is found by holding all the displacement values at zero and solving for the forces caused only by self straining.

## Beams

A beam is defined as having torques and forces, perpendicular to its length, acting on it (there are no axial forces). At each end node of the beam there is now a force,  $Q_{2i-1}$ , and a torque,  $Q_{2i}$ . Likewise, there is a displacement,  $q_{2i-1}$ , and an angle of rotation,  $q_{2i}$ . The unrestrained stiffness matrix is

$$[K] = EI \begin{bmatrix} \frac{12}{L^3} & -\frac{6}{L^2} & -\frac{12}{L^3} & -\frac{6}{L^2} \\ -\frac{6}{L^2} & \frac{4}{L} & \frac{6}{L^2} & \frac{2}{L} \\ -\frac{12}{L^3} & \frac{6}{L^2} & \frac{12}{L^3} & \frac{6}{L^2} \\ -\frac{6}{L^2} & \frac{2}{L} & \frac{6}{L^2} & \frac{4}{L} \end{bmatrix} \quad (2.44)$$

The  $[K]$  matrix is again used to solve for the unknown displacements and angles of rotation. These values can then be used to determine the bending moment and shearing force in the beam at any point along the beam. The direction along the beam is labeled as the Z-axis.

$$\begin{bmatrix} V_1(z) \\ M_1(z) \end{bmatrix} = EI \begin{bmatrix} -\frac{12}{L^3} & \frac{6}{L^2} & \frac{12}{L^3} & \frac{6}{L^2} \\ \frac{6}{L^2} - \frac{12z}{L^3} & -\frac{4}{L} + \frac{6z}{L^2} & -\frac{6}{L^2} + \frac{12z}{L^3} & -\frac{2}{L} + \frac{6z}{L^2} \end{bmatrix} \begin{bmatrix} q_1 \\ q_2 \\ q_3 \\ q_4 \end{bmatrix} \quad (2.45)$$

## Frames

A frame combines trusses and beams in that it contains a force parallel to the length of the bar, a force perpendicular to the length of the bar, and a torque. A capital Q is used to distinguish the forces and torques, while the lower case q is used to name the displacements and angles of rotation. Each end node has three degrees of freedom which are  $3i$ ,  $3i - 1$ , and  $3i - 2$  where  $i$  is described in Figure 3.3.3. The unrestrained stress matrix for a frame is



most common causes of failure are improper material selection and processing, inadequate design of components, and misuse of components. Thus, material selection is an important process in the design of a structure. If failure should occur it is up to the engineer to learn the causes in order to prevent them from happening in the future.<sup>5</sup>

All materials contain large numbers of defects or imperfections. In fact, the material's properties are sensitive to deviations from a flawless crystalline structure. Classification of crystalline imperfections are frequently made according to the geometry and the dimensions of the defect. There are several types of defects including: point defects (those associated with one or two atomic positions), linear (or one-dimensional) defects, and interfacial defects or boundaries which are two-dimensional. Impurities are considered point defects.<sup>5</sup> A factor of safety is used to account for these errors.

Most materials experience some type of interaction with a large number of diverse environments. Often, such interactions impair a material's usefulness as a result of the deterioration of its mechanical properties, other physical properties, or appearance. Deteriorative mechanisms are different for metals, ceramics, and polymers. In metals there are actual material losses either by dissolutions (corrosion) or by the formation of nonmetallic scales or films (oxidation). Ceramic materials are relatively resistant to deterioration, which usually occurs at elevated temperatures or in a rather extreme environment. Polymers mechanisms and consequences differ from those of metals and ceramics, and the term degradation is used. Polymers may dissolve when exposed to a liquid solvent, or they may absorb the solvent and swell. Also, heat and electromagnetic radiation may cause alterations in a polymer's molecular structure.<sup>5</sup>

Although the electrical properties of materials in the structure are not the main determining factor for material selection, basic electrical properties are useful to know. One of the most important electrical characteristics of a solid material is the ease with which it transmits an electric current. Ohm's law relates the current to the applied voltage:

$$V = IR \tag{2.48}$$

where  $R$  is the resistance,  $I$  is the current,  $V$  is the voltage, The resistivity  $\rho$  is independent of the specimen geometry but related to  $R$  through the expression that is given by:

$$\rho = \frac{RA}{l} \tag{2.49}$$

where  $l$  is the distance between the two points at which the voltage is measured.  $A$  is the cross-sectional area perpendicular to the direction of the current.  $\sigma$  is the electrical conductivity that is used to specify the electrical character of a material. It is the reciprocal of the resistivity and is given by:

$$\sigma = \frac{1}{\rho} \quad (2.50)$$

where  $\sigma$  is the electrical conductivity and  $\rho$  is the resistivity. The electrical conductivity is an indication of the ease with which a material is capable of conducting an electric current.

Thermal properties are the response of a material to the application of heat. As a solid absorbs energy in the form of heat, its temperature rises and its dimensions increase. The energy may be transported to cooler regions of the specimen if the temperature gradient exists, and ultimately, the specimen may melt. Heat capacity, thermal expansion, and thermal conductivity are properties that are critical in the practical utilization of solids. Heat capacity is a property that is indicative of the ability of the material to absorb heat from the external surroundings.<sup>5</sup> It represents the amount of energy required to produce a unit temperature rise and it is given by:

$$C = \frac{dQ}{dT} \quad (2.51)$$

where  $dQ$  is the energy required to produce a  $dT$  temperature change. Most solid materials expand upon heating and contract upon cooling. The change in length with temperature for a solid material is given by:

$$\frac{l_f - l_0}{l_0} = \alpha_l(T_f - T_0) \quad (2.52)$$

or

$$\frac{\Delta l}{l_0} = \alpha_l(\Delta T) \quad (2.53)$$

where  $l_0$  and  $l_f$  represent the initial length and final length respectively, with the temperature change from  $T_0$  to  $T_f$ . Parameter  $\alpha_l$  is the linear coefficient of thermal expansion; it is a material property that is indicative of the extent to which a material expands upon heating, but heating or cooling affects all the dimensions of a body, with a resultant change in volume. Volume changes with temperature are given by:

$$\frac{\Delta V}{V_0} = \alpha_v(\Delta T) \quad (2.54)$$

where  $\Delta V$  and  $V_0$  are the volume change and the original volume respectively and  $\alpha_v$  symbolizes the volume coefficient of thermal expansion.

Thermal conduction is the phenomenon by which heat is transported from high-to-low temperature regions of a solid. The property that characterizes the ability of a material to transfer heat is the thermal conductivity and is given by:

$$q = -k \frac{dT}{dx} \quad (2.55)$$

where  $q$  is the heat flux or heat flow,  $k$  is the thermal conductivity and  $dT/dx$  is the temperature gradient through the conducting material.

Thermal stresses are stresses induced in a body as a result of changes on temperature. Thermal stresses are given by:

$$\sigma = E\alpha_l(T_0 - T_f) = E\alpha_l\Delta T \quad (2.56)$$

where  $E$  is the modulus of elasticity and  $\alpha_l$  is the linear coefficient of thermal expansion.

Magnetism is the phenomenon by which materials assert an attractive or repulsive force or influence on other materials. The externally applied magnetic field strength is given by:

$$H = \frac{NI}{l} \quad (2.57)$$

where  $H$  is the magnetic field strength,  $N$  is the number of turns in a coil, and  $l$  is the length of the coil carrying a current  $I$ . These labels are illustrated in Figure 2.10. The relationship between the magnetic field strength and the flux density is given by:

$$B = \mu H \quad (2.58)$$

where the parameter  $\mu$  is the permeability, which is a property of the specific medium through which the  $H$  field passes and in which  $B$  is measured.

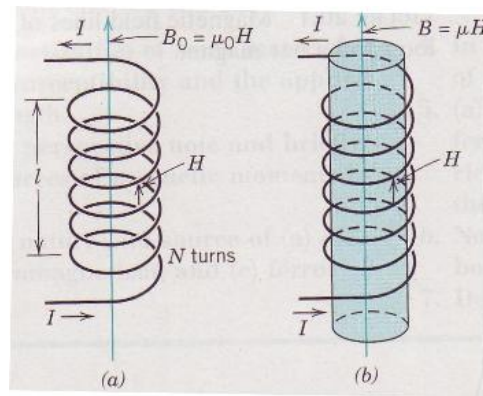


Figure 2.10: Magnetic Field and Magnetic Flux in a Coil<sup>5</sup>

Optical properties of a material are the material's response to exposure to electromagnetic radiation. The spectrum is illustrated in Figure 2.11. The main concern is whether the material allows radiation or visible light to pass through it.

Mechanical properties of materials are the most relevant for the construction of a structure. The density of a material is related to the mass and volume of that material and is given by:

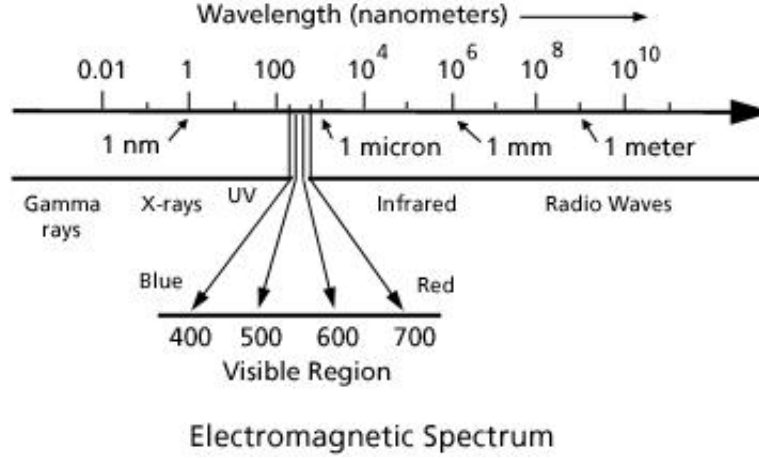


Figure 2.11: Spectrum of Electromagnetic Waves<sup>5</sup>

$$\rho = \frac{m}{V} \quad (2.59)$$

where  $\rho$  is the density,  $m$  is the mass, and  $V$  is the volume. The mass of a structure needs to be minimized, in order to make the structure as light as possible. However, the structure needs to fulfill the other design criteria; therefore, a light-weight material may not be suitable for all applications as illustrated in Figure 2.12.

When stress and strain are proportional to each other the material is said to be experiencing elastic deformation; otherwise the material is experiencing plastic deformation, that is Hooke's law does not apply. In the elastic region the material will return to its original shape, whereas in the plastic region the material is permanently deformed as illustrated in Figure 2.13.

Young's modulus is the slope of Figure 2.13. The higher the value of Young's modulus, the higher the stress per strain ratio. In most cases high values of Young's modulus are preferable for structural materials so that large loads can be applied and minimal deflection will be experienced by the material.

When an axial load is applied to a metal specimen there will be an elastic elongation and an axial strain. The elastic elongation will produce constrictions in the lateral strains. Poisson's ratio,  $\nu$ , is defined as the ratio of the lateral and axial strains in an object and is given by:

$$\nu = -\frac{\epsilon_{transverse}}{\epsilon_{longitudinal}} \quad (2.60)$$

where  $\nu$  is Poisson's ratio,  $\epsilon_{transverse}$  is the strain in the direction transverse direction and  $\epsilon_{longitudinal}$  is the strain in the longitudinal direction as illustrated in Figure 2.14.

The maximum value for Poisson's ratio is 0.50 as long as there is no volume change, and the value is 0.25 for isotropic materials. Using Poisson's ratio, lateral strains can be determined along with axial strains, which are important to the stress of the

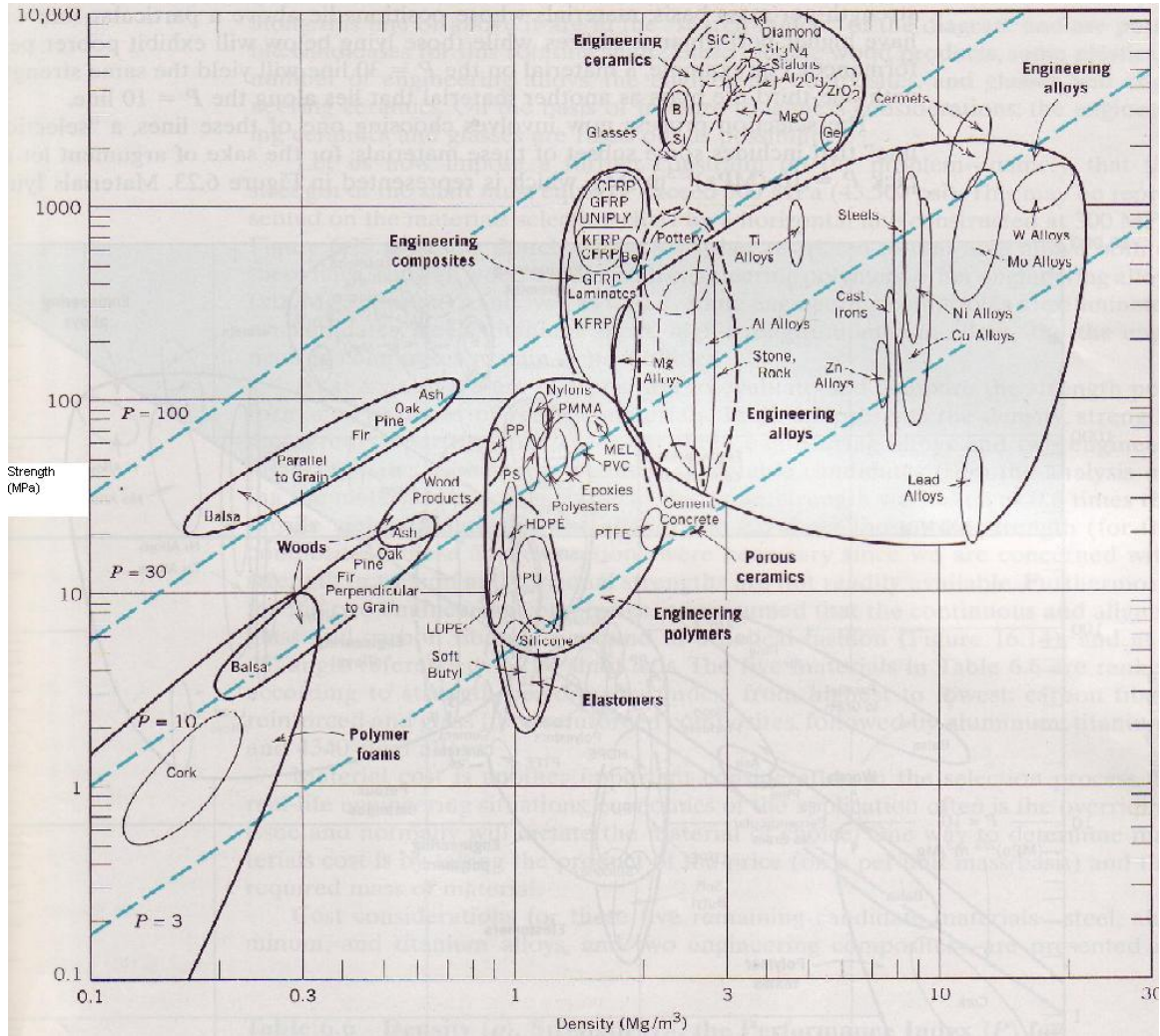


Figure 2.12: Strength as a Function of Density<sup>5</sup>

material. The shear modulus is also related to Young's modulus through Poisson's ratio. The shear modulus is similar to Young's modulus, in that it relates a stress to a strain, and is given by:

$$E = 2G(1 + \nu) \quad (2.61)$$

where  $G$  is taken to be 40% of Young's modulus. The shear modulus relates shear stress to an angle of twist and is given by:

$$\tau = G\theta \quad (2.62)$$

where  $\tau$  is the shear force and  $\theta$  is the angle of twist.

The strength of a material is important to the design of a structure. The deter-

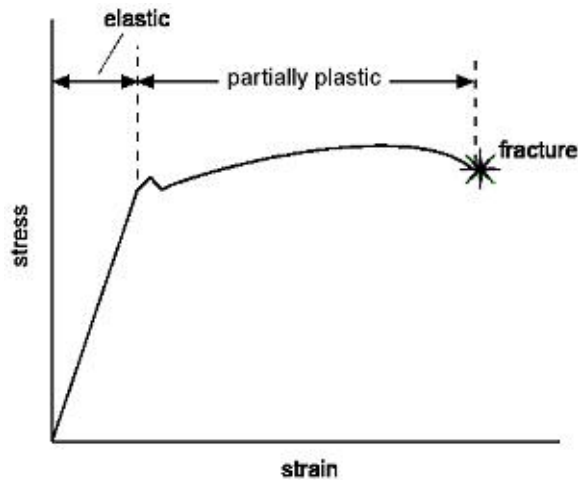


Figure 2.13: Stress-Strain Graph

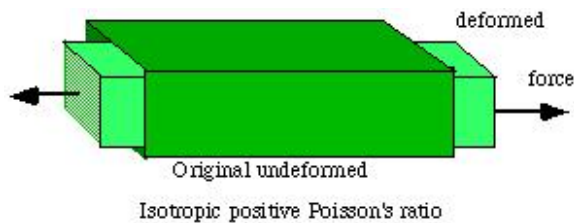


Figure 2.14: Isotropic Positive Poisson's Ratio

mining strength property for metals is the yield strength, which is the region where the material experiences plastic deformation as illustrated in Figure 2.13. The yield stress for a material is the maximum stress the material can withstand before yielding. A factor of safety is implemented in the equation to find the maximum stress allowable for the structure and thus is given by:

$$\sigma_{max} = \frac{\sigma_y}{FS} \quad (2.63)$$

where  $\sigma_{max}$  is the maximum stress,  $\sigma_y$  is the yield stress and  $FS$  is the factor of safety.

The fracture toughness of a material is a measure of a material's resistance to brittle fracture when a crack is present. The length of the crack is determined depending on whether the crack is in the middle of the specimen or on the edge as illustrated in Figure 2.15.

The fracture toughness is given by:

$$K_c = Y\sigma_c\sqrt{\pi a} \quad (2.64)$$

where  $K_c$  is the fracture toughness,  $Y$  is a dimensionless parameter which has a value of approximately unity,  $\sigma_c$  is the critical stress required for the crack to propagate,

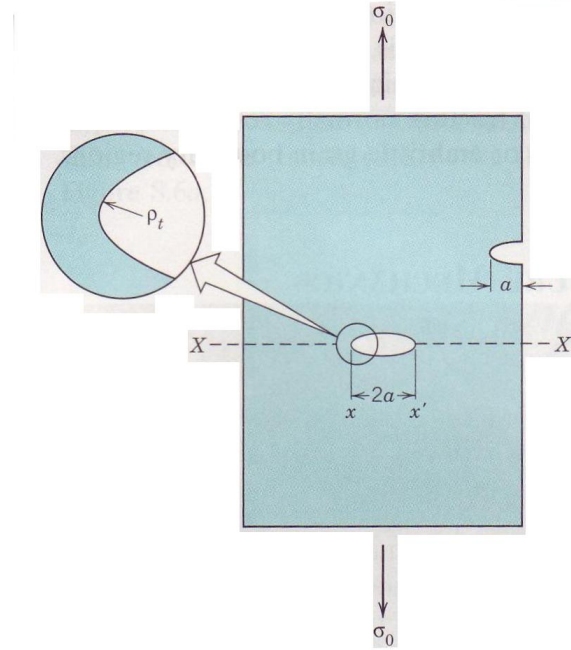


Figure 2.15: The geometry of surface and internal crack<sup>5</sup>

and  $a$  is one half the length of an internal crack. The critical stress is given by:

$$\sigma_c = \sqrt{\frac{2E\gamma_s}{\pi a}} \quad (2.65)$$

where  $\gamma_s$  is the specified surface energy.

Ductility is the measure of the degree of plastic deformation that will be sustained at fracture. If the material experiences very little or no plastic deformation at all then it is termed a brittle material. The two quantities that represent ductility are percent elongation and percent reduction in area and are given by:

$$\%EL = \frac{l_f - l_o}{l_o} \times 100\% \quad (2.66)$$

$$\%RA = \frac{A_f - A_o}{A_o} \times 100\% \quad (2.67)$$

where  $\%EL$  is the percent elongation,  $l_f$  is the final length,  $l_o$  is the original length,  $\%RA$  is the percent reduction in area,  $A_f$  is the final area, and  $A_o$  is the original area.

Overall, material selection is important to the life and function of a structure. Many material qualities need to be taken into consideration when designing a structure, and the materials with the most desirable qualities should be chosen for the structure to have the best performance.

## 2.3 Vibrations

Shock and vibration perturbation in any mechanical or electrical device is an ongoing problem that engineers face. Engineers are constantly trying to reduce negative effects that destructive vibrations have on the proper operation of the equipment. Although professionals have developed a multitude of useful techniques for mitigation, these techniques are not applicable to every situation, specifically spacecraft.

The majority of damaging vibrations within a spacecraft actually occur during the launch process where the craft can experience shock levels in the several thousands of  $g$ 's. Massive shocks that cause such substantial forces typically occur during motor ignitions and shutdowns, stage separations, fairing separation, dual payload attach fitting separation, and spacecraft separation, which are direct results of pyrotechnic devices. The shocks subject the internal components of the spacecraft to large impulsive bursts of energy, called shock loads. These loads can be detrimental to the functionality of the craft. According to CSA Engineering, some of the known problems that result are: breakage of electrical wires and leads, breakage of solder joints, chatter of relays, cracking of pc boards and wave guides, cracking of glass diodes, potentiometer slippage, short circuits, bolt loosening, gear train fretting, buckling, and brittle fracture. Engineers are also interested in large amplitude vibrations that occur through the mission.

The major difference between a shock load and vibrations is the frequency over which the equipment tries to eliminate the problem; this difference in frequency can be seen in Figure 2.16. Vibration systems are specifically designed each mission for purposes such as launch vehicle guidance, navigation, and control as well as coupled load analysis while shock systems are slightly more generic for each mission. The following discusses possible solutions for shock and vibration mitigation during both launch and orbit.

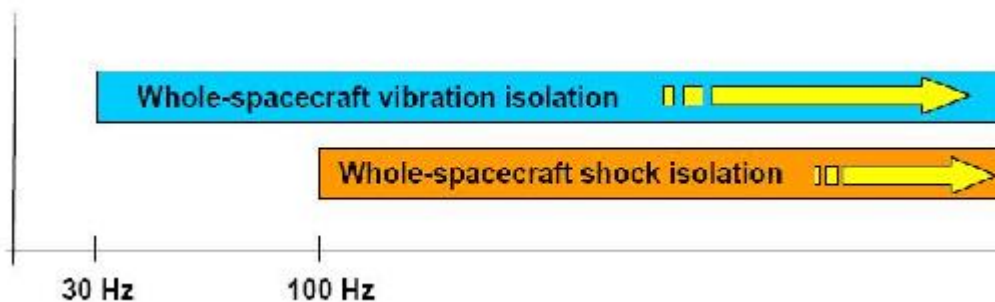


Figure 2.16: Frequency Ranges for Shock and Vibration Attenuation Systems<sup>18</sup>

### 2.3.1 Flexible Body Dynamics

The dynamics of launch are important to the design of the spacecraft and mission. As stated earlier, the largest and most damaging effects from vibrations are seen at launch. The launch itself consists of several events with various types of loading at each event. A table of events for a Titan IV launch is shown in Table 3.1 in Reference 23.

The events that may be critical to the payload and launch vehicle itself must be analyzed to ensure the success of the mission. Minimizing the effects of vibrations at launch is important to understand as well. Various equations are used to understand how to minimize these effects, including the governing equation for vibration

$$m\ddot{x}(t) + c\dot{x}(t) + kx(t) = F(t) \quad (2.68)$$

A dynamic analysis must be done in order to predict how the launch vehicle and spacecraft will respond to various forces that occur during the several events that make up the launch phase and the orbital parts of the mission. There are several ways to go about analyzing the structure as a whole. One method is to approximate everything in a single degree of freedom system, which means that the structure is modeled as a simple mass on a spring with a damper. Figure 5.1 in Reference 23 illustrates this simplification.

This simplification will not give answers that we need to design the spacecraft and launch vehicle; however, it does provide insight into the more complex problems that need to be solved to determine the actual response of the entire structure. Real structures have infinite degrees of freedom for each mode of vibration. Only the low frequency modes are of real importance though. The low frequency modes are the only type that produce a significant amount of stress. Thus, usually only a small number of vibration modes are examined. The result is the creation of a model that has as many degrees of freedom as necessary to analyze the major modes of the structure. In this method, motion is described by the equation:

$$\{x(t)\} = \sum_{i=1}^{n_m} \{\Phi_i\}q_i(t) = [\Phi]\{q(t)\} \quad (2.69)$$

where  $x(t)$  is the vector of displacements for the DOFs (degrees of freedom) as a function of time,  $\Phi_i$  is the vector describing the  $i$ -th modal shape;  $q_i$  is the modal coordinate for the  $i$ -th mode; and  $q(t)$  is the vector of modal coordinates. Table 7.2 in Reference 23 summarizes the finite-element method and the steps needed to predict the structures response to the time-varying forces. These responses are going to be the responses the entire structure encounters for the given event in launch. Thus a method of minimizing these responses must be determined.

There are two major methods of reducing the vibrations encountered during launch itself. One method is to find a way to reduce the dynamic launch loads encountered by the structure. The other method is to stiffen the entire structure. Stiffening the

structure adds weight and thus adds to the cost of the mission; however, if the loads are reduced then the weight requirement is lessened. So, a combination of the two methods is most desirable. As the loads are reduced, the structure can be stiffened accordingly to reduce the vibrations even more.

### 2.3.2 Orbital Vibration Mitigation

Although orbital vibrations are easily kept quite minimal using basic dampening technologies, sometimes they can cause major problems. Multiple instruments and sensors aboard spacecraft are used to gather information from distant places that can be hundreds of millions of kilometers away. When measurements like the former are being conducted, any slight vibration can cause substantial noise within the signal leading to corrupted data. Some of the possible sources of vibration that a satellite can encounter while in orbit are: reaction wheels, solar array drives, cryogenic coolers, and vibrations from host components. Ultimately, the vibrations lead to decreased performance on both instruments and sensors; although there are filtering processes that can correct the problem, the vibrations still need to be minimized.

One type of vibration isolation system being tested is the Satellite Ultraquiet Isolation Technology Experiment (SUITE), which is a "piezoelectric-based technology". Figure 2.17 portrays a photograph of the constructed system of six active/passive struts used for vibration isolation. Each strut can provide passive vibration isolation above  $28Hz$  and can also be reprogrammed to implement multiple control algorithms. The SUITE system can also reduce radial vibration perturbation using active control to reduce response in to the  $5 - 100Hz$  range.

A major problem with the use of cameras and other imaging devices aboard a spacecraft is the fact that the images often become quite distorted when viewing objects from a substantial distance. "Slight hums within the craft cause the image to seem blurring and out of focus" according to a Phd candidate of Dr. Dale A. Lawrence at the University of Colorado - Boulder. There Dr. Lawrence and his team are currently investigating possible ways of mitigating small vibrations within spacecraft and have developed a quite intriguing idea. That idea is to position a camera on the surface of a separate body not connected to the spacecraft. When the camera needs to be repositioned, the body will secure itself to the spacecraft and relocate the camera. Once the camera has locked in on its target, the body, connected only by a short retractable cable, frees itself from the spacecraft. This implementation allows the body and the camera to freely move in space, while not being affected by the spacecraft vibrations, other than those that resonate within the camera itself.

The large shock and vibration responses can result from various processes that occur before, during, and after launch. Although some seem quite trivial, their effect on the system needs to be considered. All possible approaches are taken to reduce the effects of shock and vibration within the spacecraft in order to ensure a successful mission. One slight, impulsive shock can make the spacecraft crash. To guarantee

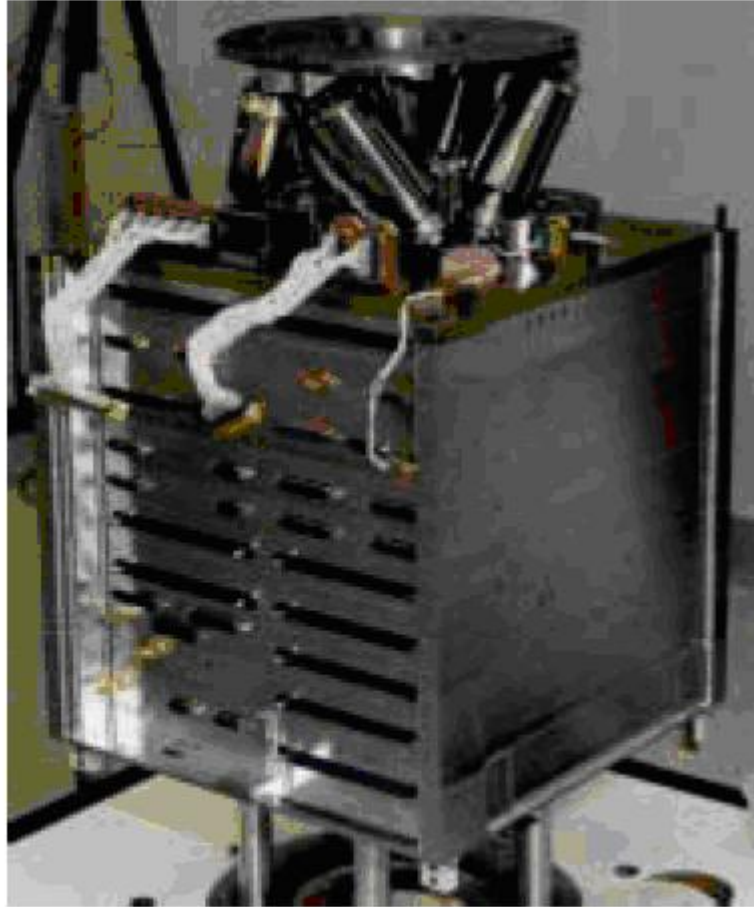


Figure 2.17: Reusable magnetic isolation system<sup>10</sup>

the safety of society and the proper operation of all equipment aboard the spacecraft, proper steps for vibration mitigation within the spacecraft, specifically during launch will be detailed.

### **2.3.3 Vibrations Summary**

Any vibration that a system endures could cause failure, thus costing time and money. To avoid this minimizing the various vibrational sources is key. One of these sources of vibration is the Launch Vehicle Adapter, which will be discussed in the next section.

## **2.4 Launch Vehicle Connector**

The Launch Vehicle Adapter (LVA) is the part of the launch vehicle that connects the launch vehicle to the spacecraft, and must be able to absorb the largest lift-off

forces without damaging the spacecraft. When designing the LVA, the design team must know the dimensions and criteria for the launch vehicle including: gross vehicle weight, propellant weight, section weights, thrust at lift-off, length and diameter of sections, and materials that the launch vehicle will be made of.

The design of the LVA includes many factors. Most important of these factors is the maximum load  $n_{max}$  because that is the maximum load the spacecraft will be under. Shown in this section is the derivation of  $n_{max}$ .

### 2.4.1 Launch Vehicle Theory

In order to properly discuss the LVA, the theory behind solving the problem must be discussed. This theory includes developing a Consistent Mass Matrix (CMM) using structural dynamics for a beam and later expanding it for the launch vehicle.<sup>23</sup>

#### Consistent Mass Matrix

Using structural dynamics to consider a uniform bar with a length  $l$ , cross-sectional area  $A$ , modulus of elasticity  $E$ , and a mass density denoted by  $\rho$ . The bar is subjected to an axial force  $N(x, t)$ , where  $x$  is the axial coordinate defined as  $0 \leq x \leq l$  and the displacement of the bar is defined as  $u(x, t)$ . It is possible to relate  $N(x, t)$  and  $u(x, t)$  for the free body element of infinitesimal length  $\partial x$  at a time instant  $\partial t$  which is given by:<sup>23</sup>

$$\frac{\partial N}{\partial x} = \rho A \frac{\partial^2 u}{\partial t^2} \quad (2.70)$$

By integrating the left hand side from 0 to  $l$  and letting  $N(0) = -F_1$  and  $N(l) = F_2$  the equation can be can be solved for  $F_1$  and  $F_2$  using structural dynamics.

$$F_1 = k(u_1 - u_2) + \left( \frac{m}{3} \ddot{u}_1 + \frac{m}{6} \ddot{u}_2 \right) \quad (2.71)$$

$$F_2 = k(u_2 - u_1) + \left( \frac{m}{6} \ddot{u}_1 + \frac{m}{3} \ddot{u}_2 \right) \quad (2.72)$$

$$(2.73)$$

where  $k$  is defined as the spring stiffness  $k = \frac{EA}{L}$  and the mass of the bar is  $m = \rho AL$ ,  $u_1$  is the nodal displacement at the beginning of the bar,  $u_2$  is defined as the nodal displacement at the end of the bar, and  $\ddot{u}_1$  and  $\ddot{u}_2$  are the accelerations at the end and beginning of the bar. In order to find the various  $k$ 's, the cross-sectional area,  $A$ , of the centaur ,if applicable, must be found. In order to find  $A$ , the thickness of the centaur shell wall must be found using the equation given by:<sup>23</sup>

$$W = 2\pi L t_w \nu \quad (2.74)$$

where  $t_w$  is the wall thickness,  $W$  is the weight of the centaur where applicable,  $L$  is the length of the centaur, and  $\nu$  is the specific weight of the material being used. The CMM can now be constructed by separating  $F_1$  and  $F_2$  into matrices given by:<sup>23</sup>

$$\begin{bmatrix} F_1 \\ F_2 \end{bmatrix} = \begin{bmatrix} k & -k \\ -k & k \end{bmatrix} \begin{bmatrix} u_1 \\ u_2 \end{bmatrix} + \begin{bmatrix} \frac{m}{3} & \frac{m}{6} \\ \frac{m}{6} & \frac{m}{3} \end{bmatrix} \begin{bmatrix} \ddot{u}_1 \\ \ddot{u}_2 \end{bmatrix} \quad (2.75)$$

### 2.4.2 Expanding the CMM

As the the beam was expanded in the previous section to the launch vehicle case, the force side of the equation for the CMM will include four forces. With a launch vehicle, the only force being applies during lift-off is at the bottom of the booster and that will be called  $F_1$ . The rest of the force matrix will be zeros and therefore the CMM for a launch vehicle can be given by:<sup>20</sup>

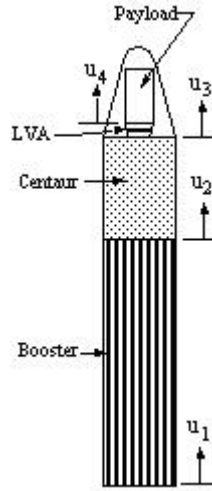


Figure 2.18: Description of Rocket DOF<sup>20</sup>

$$\begin{bmatrix} F_1 \\ 0 \\ 0 \\ 0 \end{bmatrix} = \begin{bmatrix} \frac{m_1}{3} & \frac{m_1}{6} & 0 & 0 \\ \frac{m_1}{6} & \frac{(m_1+m_2)}{3} & \frac{m_2}{6} & 0 \\ 0 & \frac{m_2}{6} & \frac{m_2}{3} + m_3 & 0 \\ 0 & 0 & 0 & m_4 \end{bmatrix} \begin{bmatrix} \ddot{u}_1 \\ \ddot{u}_2 \\ \ddot{u}_3 \\ \ddot{u}_4 \end{bmatrix} + \begin{bmatrix} k_1 & -k_1 & 0 & 0 \\ k_1 & k_1 + k_2 & -k_2 & 0 \\ 0 & -k_2 & k_2 + k_a & -k_a \\ 0 & 0 & -k_a & k_a \end{bmatrix} \begin{bmatrix} u_1 \\ u_2 \\ u_3 \\ u_4 \end{bmatrix} \quad (2.76)$$

where  $m_i$ ,  $k_i$ ,  $u_i$ , and  $\ddot{u}_i$  are defined as the booster for  $i = 1$ , the centaur for  $i = 2$ , the LVA for  $i = 3$ , and the payload is defined as  $i = 4$ .  $k_a$  is the spring constant of the LVA.<sup>20</sup>

This matrix equation can then be treated as a differential equation and solved accordingly. The matrix  $[M]$  is the mass matrix and  $[K]$  is the spring constant matrix from equation (2.76), so the simplified equation is given by:

$$\{F\} = [M]\{\ddot{u}\} + [K]\{u\} \quad (2.77)$$

with a solution that is more simple with coordinate transfer. The modal vector matrix  $[\Phi]$  is used to get  $[M_g]$  and  $[K_g]$  which are the mass matrix and spring constant matrix respectively. Solutions are given by:<sup>20</sup>

$$[K]\{\phi\} - \lambda[M]\{\phi\} = 0 \quad (2.78)$$

$$\{u\} = [\Phi]\{q\} \quad (2.79)$$

$$[M_g] = [\Phi]^T[M][\Phi] \quad (2.80)$$

$$[K_g] = [\Phi]^T[K][\Phi] \quad (2.81)$$

$$[F_g] = [\Phi]^T[F] \quad (2.82)$$

Using an eigenvalue function solver, the values of  $[\Phi]$  and  $\lambda$ , where  $\lambda$  is the modal values of the equation, can be obtained. After the transformation to the new coordinate system, the new differential equation is given by:<sup>20</sup>

$$[M_g]\{\ddot{q}\} + [K_g]\{q\} = \{F_g\} \quad (2.83)$$

The natural frequency,  $\omega_i$  of the launch vehicle at the different sections can be obtained from  $[K_g]$ . For example  $\omega_2 = \sqrt{[K_g]_{(2,2)}/[M_g]_{(2,2)}}$ . Equation (2.83) can be solved to give four different  $q$ 's, where  $t$  is the time in seconds.<sup>20</sup>

$$\{q\} = \{F_g\} \begin{bmatrix} t^2 \\ (1 - \cos \omega_2^2 t)/\omega_2^2 \\ (1 - \cos \omega_3^2 t)/\omega_3^2 \\ (1 - \cos \omega_4^2 t)/\omega_4^2 \end{bmatrix} \quad (2.84)$$

The maximum loading factor can be determined over a given time frame after lift-off. The maximum loading factor  $n_{max}$  is given by:

$$n_{max} = 1 + \ddot{u}_{max}/g \quad (2.85)$$

where  $\ddot{u}_{max}/g$  is the maximum acceleration at the payload divided by gravity. Solving equation (2.83) for  $\ddot{q}$  and then using the same conversion used in equation (2.79),  $\{\ddot{u}\}$  is found. A simple iterative program can be used to find the maximum value for  $\ddot{u}_4$ . The number one added in Equation 2.85 is the weight of the payload acting as a loading factor upon itself.<sup>20</sup>

### 2.4.3 Launch Vehicle Summary

The  $n_{max}$  that has been derived is the maximum loading factor that the LVA will undergo for a given time frame and thus the LVA can be designed accordingly. This is an overly-simplified model, but is a good approximation for the actual design. In the real world, the design team would make the process more accurate by taking more than four points.

## 2.5 Summary

The analysis of a spacecraft's structure can be simplified to the analysis of critical points. The critical points are the areas of the structure that experience the maximum stress. These points are analyzed to determine the size, shape, and material of that structural component. The stresses are caused by vibrations that the spacecraft experiences. These vibrations are generally caused during lift-off and therefore the stresses reach a maximum during this period. Since the vibrational analysis determines the maximum stresses, they also determine the materials used for the structure. The material is chosen to withstand stresses, fracturing, and its resistiveness to the thermal effects of space. The next chapter will discuss examples of actual materials and mechanisms used in a spacecraft along with costs, manufacturer and vendor choices, size and weight, and other detailed information pertaining to real spacecraft components.

# Chapter 3

## Technologies and Examples

An engineer must know what components are available in order to design a spacecraft. Information such as who makes the component, how much does it cost, what is its mass and volume, and has it been used in space before can help an engineer choose which component is the best. Chapter 3 answers these questions for structures, mechanisms, launch vehicles, and new technology. The last section of chapter 3 has examples that show how the equations in chapter 2 are used to determine material criteria for choosing components.

### 3.1 Available Technologies

The available structural components are broken into beams, mechanisms, and launch vehicles. Beams can be made out of various materials ranging from titanium to plastics. Structural mechanisms allow the spacecraft to expand once in orbit and help release the payload from the launch vehicle. The choice of launch vehicle depends on the payloads specifications, launch trajectory, and the type of mission.

#### 3.1.1 Available Launch Vehicles

There are many launch vehicles available around the world. It is important to find the proper launch vehicle for the desired mission. This section has narrowed down the large list to seven groups of launch vehicles. The launch vehicles examined each have their own qualities that might be crucial to the success of a mission. The table below lists the launch vehicles examined in this section and some of their important characteristics that would need to be analyzed to select the proper launch vehicle.

##### **Atlas**

The Atlas family of launch vehicles is produced by Lockheed-Martin Space Systems. There are only three family members in current operation: the Atlas IIAS, III, and V.

Launch Vehicle Type	Primary Mission Destination	Launch Site	inclination angles available (degrees)	largest mass(kg) to GTO
Atlas IIAS	GTO	Cape Canaveral, FL Vandenberg AFB	28.5 - 55 63-120	3719
Atlas IIIA	GTO	Cape Canaveral, FL	28.5 - 55	4037
Atlas IIIB	GTO	Cape Canaveral, FL	28.5 - 55	4119
Atlas V400	GTO & GEO	Cape Canaveral, FL	28.5 - 55	4970
Atlas V500	GTO & GEO	Cape Canaveral, FL	28.5 - 55	8670
K-1	LEO	Woomera, Australia Nevada Test Site	45 - 60; 84 -99	1570
Delta II	GPS;LEO; deep space	Cape Canaveral, FL Vandenberg AFB	28.5 - 60 63 - 145	1832
Delta IV medium	GPS;LEO; deep space	Cape Canaveral, FL Vandenberg AFB	28.5 - 51 63 - 120	4231
Delta IV heavy	GPS;LEO; deep space	Cape Canaveral, FL Vandenberg AFB	28.5 - 51 63 - 120	12757
Pegasus	small commercial (LEO)	Cape Canaveral, FL Vandenberg AFB Wallops Flight Facility Reagan Test Center	28-58 70-130 30-65 11 to 18	not capable
Taurus SSLV	LEO and GTO	Cape Canaveral, FL Vandenberg AFB	28.5 - 40 55 - 120	400
Taurus XL	LEO and GTO	Cape Canaveral, FL Vandenberg AFB	28.5 - 40 55 - 120	495
Taurus Commercial	LEO and GTO	Cape Canaveral, FL Vandenberg AFB	28.5 - 40 55 -120	557
Ariane 5G	GTO	Guiana Space Center	5.2 - 100.5	6700
Ariane 5ECA	GTO	Guiana Space Center	5.2 - 100.5	10500
Zenit 2SLB	LEO	Baikonur LC	51.4 - 63.9	4900
Zenit 3SL	GTO	Baikonur LC	51.4 - 63.9	3500
Zenit 3SLB	GTO	Baikonur LC	51.4 - 63.9	6066
		Odyssey launch platform(mobile)ALL		
		Baikonur LC	51.4 - 63.9	
		Odyssey launch platform(mobile)ALL		

Figure 3.1: Table of Launch Vehicle Data<sup>15</sup>

The Atlas III and V each have two different active models; The Atlas III has models IIIA and IIIB and the Atlas V has models V400 and V500. Each of the models vary in both size and capability.

The Atlas IIAS is primarily used for medium sized commercial and government satellite launches to GTO. It improves upon the Atlas IIA model by the addition of solid strap-on boosters, but the Atlas IIAS is currently being phased out in favor of the Atlas V. The Atlas III provides a higher performance than the Atlas IIAS primarily due to a single Russian RD-180 engine that has replaced the Atlas II's main propulsion system. The RD-180 engine is self-contained and allows the elimination of the half-stage booster separation. Typical use of the Atlas III launch vehicle is to carry medium-sized commercial or government spacecrafts into GTO. Capabilities of the Atlas III include the ability to launch up to a 4119 kg payload to GTO. Limiting factors for the Atlas III include the inability to send a spacecraft into either Sun-Synchronous Orbit or Geostationary Orbit. The Atlas III has two variations: the Atlas IIIA and IIIB. The Atlas IIIB has a longer Centaur than its family counterpart in order to use one of two different engines for increased performance for entering GTO. For example, the Atlas IIIB has a payload weight capability of 9239 kg to a 407 km orbit, which is nearly 1500 kg more than the Atlas IIIA can carry. Launch

cost for a known Atlas IIIB has been listed at around \$70.7 million.

The Atlas V series is a result of new U.S. government demands for new launch services. Differentiating the Atlas V from the Atlas III is a new first-stage design called the common core booster that still uses the RD-180 engine. The common core booster is basically a reinforced first stage structure with increased propellant. The Atlas V is made up of two designs. The Atlas V400 series uses the same fairing as the Atlas III, which is 4 meters in diameter. The V400 has made improvements so that it can use three solid strap-on boosters for increased thrust. The Atlas V500 series has a new 5 meter diameter payload fairing with the ability to use five strap-on boosters. Solid rocket boosters enable the Atlas V to meet varied performance requirements for missions ranging from LEOs to geosynchronous orbits. The Atlas V500 series has a larger capability because it can carry payloads of 8670 kg to GTO, which is 4950 kg more than the V400. The cost range for Atlas V is known to be between \$75 and \$110 million for a medium-class spacecraft.<sup>15</sup>

## **K-1**

The K-1 is a two-stage reusable launch vehicle developed by Kistler Aerospace Corporation. The system design is driven by the desire to reuse the vehicle and create a low cost launch vehicle. The vehicle is designed to bring spacecraft into Space Station Orbit, Sun-Synchronous Orbit, GTO, and Geostationary Orbit. Liquid-propellant engines power the vehicle for the first and the second stages. Costs of the missions to LEO are priced at \$17 million per flight, whereas missions that require an expendable upper stage for higher altitude orbits are priced at \$25 million.

The stages of the K-1 burn RP grade kerosene and LOX, which avoid complexities that can be caused by a hydrogen-fueled system. These propellants are nontoxic and easier to maintain than other systems, which is essential for a reusable launch vehicle. Each stage includes a propulsion system, a composite airframe, and propellant tanks. The first stage includes a smaller LOX retention tank so that it can return to the launch site. All remaining propellant from the main tank will evaporate in the pitch maneuver.

The K-1 avionics systems are unique because both stages have their own control systems for independent flight. Also the second stage must power down for 18 hours in orbit to conserve power before returning to the launch site. The result of the high reliability needed is that the guidance and control systems are triple-redundant and fault tolerant. Navigation data for the control systems are provided by three GPS systems called EGIs, which combines the GPS receivers with inertial measurement units in order to provide accurate control of the launch vehicle.

The payload module is a separate element of the launch vehicle, which completely encloses and protects the payload. It can be removed from the vehicle after landing to support processing and encapsulation of the next payload away from the rest of the vehicle preparations. The module is available in two sizes, both with diameters

of 4.3 meters. The extended payload module differs from the standard module by a length of 5.9 meters compared to 3.5 meters.<sup>15</sup>

## **Delta**

The Delta family of launch vehicles has two members which are the Delta II and the Delta IV. The Delta II is available in a two-stage or three-stage model. The primary mission of the two-stage model is to launch remote sensing, research, and LEO communications satellites. The primary mission of the three-stage model is to launch DPS satellites and deep-space missions. The 7420 series and the 7320 series use either three or four strap-on motors, depending on the size of the payload. The 7925 series uses nine strap-on motors for medium-sized payloads. The 7925H series is the newest configurations, and uses nine strap-on motors, including 3 larger strap-on motors, and will be able to launch heavier payloads.<sup>15</sup>

The Delta II has two different possible launch sites. It can be launched from the Cape Canaveral AFS, and Vandenberg AFB. The two launch sites provide a wide range of available launch inclinations. The Delta II also has a flight rate between three and twelve launches per year.<sup>15</sup>

The Delta IV has two variations: Medium and Medium Plus, which have been operational since 2002. The primary missions of these launch vehicles are the same as of the Delta II. The Delta IV Medium is capable of launching payloads as large as 9,144 kg. The Delta IV Medium Plus can handle payloads as large as 13,701 kg. The Delta IV Heavy is still in development, but it is expected to deliver payloads up to 23,975 kg into a 185 km orbit and payloads of up to 6,276 kg directly into GEO. It will also be capable of launching earth escape missions.<sup>15</sup>

The Delta IV launch vehicle is capable of launching heavier payloads into the same orbits as the Delta II. The Delta IV is also capable of launching lighter payloads into GEO. The Delta IV may be launched from the same launch sites as the Delta II at a rate of five to six launches per year.

## **Pegasus**

The Pegasus XL first came into use in 1994. Its primary mission is to carry small commercial and government payloads to LEO. It is a cost-saving design because it is able to conserve fuel by launching from an aircraft, the Orbital Carrier Aircraft (OCA), at an altitude of 12km. This approach has flaws though. It cannot carry a large payload because it has to be launched from the OCA. The maximum payload the Pegasus is able to carry is 450kg, but with a payload of this size it can only travel to 200km. This launch vehicle is able to reach an altitude of 1450km, which is a favorable asset. However, to reach this altitude the payload can only be 130kg.

The Pegasus is a good design for low orbit space missions because it is cheap and has a success rate of 84%. The cost to launch a spacecraft into space using the Pegasus XL is between 15 and 25 million dollars. The payload envelope on the

Pegasus is able to carry a 1.168m diameter by 1.11m in length cylinder payload. This size is large enough to carry most commercial satellites into space. The Pegasus can be prepared for launch in only 30 days, which makes it ideal if multiple satellites need to be launched in a small time frame.

The inclination of the spacecraft's orbit is an important factor to consider when choosing a launch vehicle. The Pegasus is able to reach almost any orbit inclination since it is launched from an OCA. The OCA must launch from an aircraft carrier that must be located in the desired strip of ocean.<sup>15</sup>

## **Taurus**

The Taurus is the ground-based sibling of the Pegasus launch vehicle which were both developed at the same time. The Taurus launch vehicle has three different iterations, the SSLV Taurus, Commercial Taurus, and Taurus XL. The first launch of the Taurus SSLV was in 1994, and the other models flew soon after. The commercial Taurus differs only slightly from the SSLV model by utilizing a Thiokol Castor. The XL model is an enhanced version of the other models. The XL uses the longer motors to power the Pegasus XL. The Taurus vehicles come at a high price. The vehicles can cost \$25-47 million. The high price has limited the Taurus to a small number of flights thus far.

The success rate for this vehicle was at a moderate level of 66.6%. With the Taurus being a ground-based rocket it can carry a a payload as large as 1310 kg; however the size of the payload can only be 2.05m in diameter and 3.31m in length.<sup>15</sup>

## **Ariane**

Ariane is one of the major European commercial satellite launch vehicles. There are only two Ariane vehicles currently available for use which are the 5G and the 5ECA models. Both models are capable of sending multiple satellites into GTO. The 5ECA model is younger and utilizes the new Vulcain 2 engine. The Vulcain 2 engine allows for more thrust, a better fuel mixture, and features a larger nozzle. The Ariane 5 project was actually designed to save money by launching multiple commercial satellites at once. The vehicle can launch up to 8 different spacecraft, with a maximum combined payload of 1200 kg. The area designed for the payload is flexible. It can be changed into a combination of four different elements to satisfy the payload's volumetric requirements. This flexibility is achieved by alternating the sizes of the payload fairing, Speltra external support structure, Sylde 5 dual payload compartment, and the ACY spacer element. Each element is chosen based upon the payload requirements needed.<sup>15</sup>

Both vehicles are relatively new. The 5G's first launch was in 1996 and has a mission success rate of about 81%; however, the rate will continue to get higher as the vehicle launches more missions. The 5ECA debuted in 2002 and has yet to be flown successfully. The estimated cost for the Ariane 5G is about 155 million dollars,

but this estimate is low. The vehicle's current cost is probably closer to the 200 to 250 million dollar range, and the 5ECA is probably around 300 to 400 million dollars. The vehicles can only be launched at the Guiana Space Center in South America. Guiana Space Center allows the Ariane launch vehicles to reach inclinations between 5.2 and 100.5 degrees.<sup>15</sup>

## **Zenit**

The Zenit launch vehicle was designed and developed in the late 1970's and early 1980's by the Soviet Union. The original purpose of the Zenit was to deliver large military satellites into LEO; however, the Zenit entered the commercial sector with the fall of the Soviet Union. There are two operational models of the Zenit launch vehicle currently available:

- 1) 2/2SLB
- 2) 3SL/3SLB

The first model is the same model that was originally used for the military satellites. The second model is a variation of the first model that is part of a joint venture led by Boeing.

The Boeing venture is commonly used for launching communication satellites. The payload accommodations are provided by Boeing and can fit a payload 11.39m long and 4.15m wide with a maximum payload of 1700 kg. The vehicle can deliver this payload into orbits up to GTO. One of the advantages that Zenit possesses is that it is made for rapid automated launches. This feature is unique for launch vehicles of this size. The success rate for the 2/2SLB model is around 84% with over 33 launches. The 3SL/3SLB model is still relatively new and has only launched 11 times, but it has over a 90% success rate. The vehicles are generally launched from Baikonur, Ukraine. The 3SL/3SLB model can also be launched at sea from a mobile launcher, which is useful for launching commercial satellites into GTO by eliminating plane changes to GEO. The cost for the launch vehicle is currently negotiable; there are no public price listings for the Zenit vehicle.

### **3.1.2 Beams**

The design of the structural components is important to the overall design of a spacecraft. One of the main structural components is a beam. When large loads are placed on a spacecraft, a beam is designed to support the structure by absorbing compressive and bending loads. The beams are designed to minimize materials while providing enough support against bending that the structural integrity is maintained. One of the more commonly used types of beams are I-beams, which support massive loads while having the strength to not buckle under loads larger than its critical load. Spacecraft beams have to support loads that may be much greater than expected at times. For this reason, titanium is used more than any other material because of its' strength to weight ratio.<sup>4</sup>

Titanium Industries, Inc. is one of the primary distributors of bulk and machined titanium. They sell types of titanium including: bars, rods, wire, plates, and blocks. Typical pricing for bulk titanium ranges from \$4 to \$11 per kg, while the pricing for machined titanium varies depending on the job.<sup>4</sup>

Other types of materials are available if the loads the structure is bearing are significant enough to not use titanium. These other materials include: carbon steel, stainless steel, brass, and aluminum. Beams made out of these materials can be purchased from the Parker Steel Company and Trident Building Systems Inc. These companies have a large selection of beam types that can be purchased or custom made. Temperature plays a vital role in choosing the right material, because of the extreme temperatures a spacecraft may face. These materials are also weaker than titanium, but with financial constraints, the sacrifice to choose a non-titanium alloy may be the only choice.<sup>4</sup>

Beams can also be made out of Carbon Reinforced Fiber Polymers (CFRP). A beam made out of CFRP is lighter weight than most metal beams, while preserving material properties comparable to those of metal. Unfortunately prices are not available for CFRP beams.<sup>4</sup>

### **3.1.3 Spacecraft Mechanisms**

In the design of a spacecraft, the selection of the required mechanisms to perform the desired tasks of the spacecraft mission becomes an important factor in the design process. Due to spacecrafts being designed for a multitude of missions, a wide variety of mechanisms will be needed. For most space missions there are three main mechanisms that stand out as the most important and necessary for spacecraft functionality. These mechanisms are: the payload release mechanisms, the solar array deployment mechanisms, and the antenna deployment mechanisms. little is known of the final size and costs of such devices, because most of these devices are constructed for the particular needs of the mission.

#### **Payload Release Mechanisms**

In order for any spacecraft to perform its mission, a launch vehicle must first launch the spacecraft into space. These launch vehicles vary in size and shape but all function to place a spacecraft into the desired orbit required of the mission. For the mission to be successful, mechanisms must be developed to deploy the spacecraft from the launch vehicle being used. These mechanisms are the most important in a spacecraft design because if the spacecraft never leaves the launch vehicle there is little or no chance for success of the mission.

Mechanisms that control the release of a spacecraft from the launch vehicle are designed to meet the needs of the particular mission. The selection of the best mechanism for the job at hand becomes a challenge, because mechanisms can only supply

but so much force on to a spacecraft to perform separation. Companies such as Alcatel and Starsys are developing a variety such mechanisms to meet such needs.<sup>7</sup>

These companies are on the forefront of the development of mechanical systems, structures, and mechanisms that open, close, release, and move components on a spacecraft. Some of these mechanisms include pin pullers, rotary actuators, hinge systems, and separation nuts. A variety of products that perform these tasks have been designed and implemented on hundreds of space missions throughout these companies lifetimes. From these products, there are two main types of mechanisms that can perform the task of releasing the spacecraft payload from the launch vehicle. These include the use of an explosive bolts release mechanism with a spring system or the more common electric signal release mechanism with spring system.<sup>7</sup>

The explosive bolts technique was widely used in the past when little care was placed on effects such an explosion would have on the spacecraft integrity. While this approach was often successful, much debris would be released into space and often the spacecraft itself experienced damage in the process. The realization of the impact of the debris in orbit has caused the technique to be phased out.<sup>7</sup>

The new approach requires the specific use of release mechanisms to avoid creating orbital debris. These mechanisms use a fast-acting separation nut that is activated by a low current signal. Normally multiple devices are used and set up in a parallel configuration. The electric signal causes a release of the bolts connecting the spacecraft to the launch vehicle. Once released, compressed springs located under the spacecraft, decompress, firing the spacecraft away from the launch vehicle.<sup>7</sup>

Many of these mechanisms have been designed to meet the needed release load ranges. Starsys alone has developed seven mechanisms, that each that have different capabilities than the rest. One mechanism is the QWKNUT 3K, which can be seen in Figure 3.2. The QWKNUT 3K is a widely used mechanism that can release loads up to 3,000 lbf (13,344 N) in a time frame of less than 35 ms. This fast release time is necessary if proper separation from the launch vehicle is to occur. Another important trait of the Qwknut is that it can be reset in under a minute by pushing a reset lever, allowing mission engineers to functionally test the same hardware that is to be used. The QWKNUT has been designed to be lightweight, only weighing 7.5 oz (200g). Key features of the Starsys QWKNUT system are that it eliminates pyrotechnic safety concerns, is lightweight and performs low-shock separation. A typical shock level for separation is under 150 g's, an order of magnitude lower than the thousands of g's that are the result of traditional explosive release bolts. Such a device was used in the release of the XSS-10 micro-satellite from the Delta-II launch vehicle. The release was a success and the micro-satellite deployment went flawlessly.<sup>7</sup>

## **Solar Array Deployment Mechanisms**

Power collection is another important part of a spacecraft's design. Power is collected by solar arrays that collect solar rays and convert them into energy. Solar arrays have

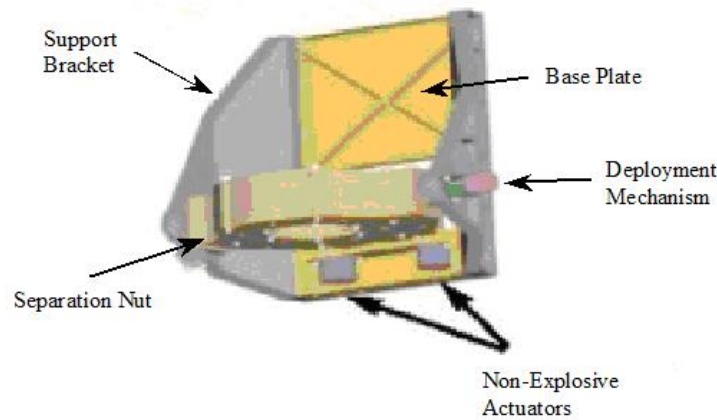


Figure 3.2: Diagram of Qwknut Mechanism<sup>7</sup>

a large area of collection in order to produce the amount of energy required by the system. Attaching such arrays directly to the spacecraft would require too much room in the launch vehicle, so these devices are normally stored as a series of folded panels hinged together.<sup>12,17</sup>

The majority of the mechanisms that attach and release the solar arrays have been designed for rapid, reliable, one-time deployment of the folded panels. One such mechanism is the Restraint, Release, and Deployment-Initiation (RRDI) device and can be seen in Figure 3.3. This mechanism was developed by the Goddard Space Flight Center the deployment of the folded arrays. The RRDI devices clamp the panels together at their hinged edges during storage, and hold them against brackets attached to the main body of the spacecraft. The brackets help to insure the panels are secure during storage. Once the RRDI device is initiated, a separation nut assembly, which is included in the RRDI device, releases the separation bolt holding the outer most panel to the spacecraft. This separation nut is similar to the design of the nuts used in the payload release process. A spring-loaded contact element located on the solar panel protrudes through the base and pushes the panels outward until fully deployed. A long leaf-spring located on the side of the separation-nut housing acts as a bumper and guides the stack of panels during deployment.<sup>12,17</sup>

Other mechanisms can also perform the task of deploying the solar array. One technique is inflating the solar array. This technique involves the use of compressed gas to fill a thin film tube which is rolled up and stored on the side of the spacecraft. The tube acts as a support for the solar panels that are attached to the side of the tube. Velcro or springs are then used to slow the unfurling of the solar array and insure proper deployment. The method is still new and needs more development.<sup>12,17</sup>

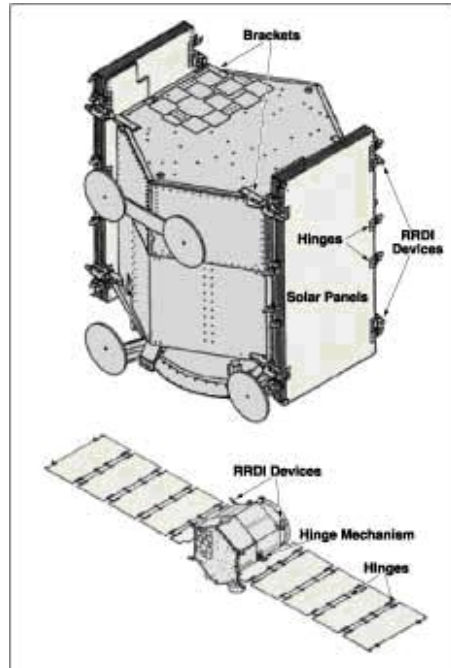


Figure 3.3: Diagram of Solar Panels Mechanisms<sup>12</sup>

### Antenna Deployment Mechanisms

Antenna deployment mechanisms are another important factor in spacecraft design. These mechanisms extend long antennas that are crucial to the spacecraft's communication capabilities. These mechanisms must be precise in their deployment to insure that the antenna is properly positioned. Other external subsystems, such as solar arrays or certain sensors, could be damaged if the antenna is deployed incorrectly.<sup>14</sup>

Two typical mechanisms used to perform this procedure are a Torsional Wheel Deployment Mechanism (TWDM) and a Spring Activated Deployment Mechanism (SADM). The TWDM was designed by a team at Stanford University. A TWDM can be compared to a tape measure, because they are both coiled around a central hub inside a housing. The difference between the TWDM and a tape measure is that the TWDM forces the antenna out of the housing by a torsional spring located inside the housing rather than being pulled out by an outside force. A large spring constant is required for the spring to deploy the antenna located in the housing. Friction-rollers are installed inside the housing to insure that the spring is able to deploy the antenna. Another mechanism that is used for the deployment is a SADM. The SADM operates by deploying a spacecraft's antenna linearly. The SADM deploys a spacecraft's antenna in a similar fashion to that of a car antenna, and it is even multisectional. Each section of the antenna fits inside the next section allowing compacted storage. Activating the SADM device allows the spring to expand, forcing the antenna setup to its fully deployed position. Locking mechanisms are used to hold the antenna in its

fully deployed position. A similar device was developed for use in a San Jose University Design Project of the micro-satellite Spartnik. The SADM are less problematic than the TWDM devices, and tend to be used where simple designs are necessary, even though this type of mechanism requires more space in the spacecraft.<sup>14</sup>

## 3.2 New Technologies

Current technologies will not be enough to further the development of space travel. The future of space travel depends on new technologies. In the near future technologies such as inflatable modules, large solar arrays, super-conducting materials, nanotubing, and flying effectors will become readily available.

### 3.2.1 Inflatable Structures

Mass is a significant constraint when traveling into space. The mass of the payload limits which launch vehicle can be chosen. One way to reduce the payload's mass is to make the structure out of inflatable materials.

#### Background

Goodyear was the first to research the idea of inflatable structures. During the 1950's and 1960's Goodyear developed inflatable structural concepts for a radar antenna, a radar calibration sphere, and a lenticular inflatable parabolic reflector. The inflatable radar antenna is based on the idea of a rigidizable support structure and a metallic mesh for the aperture surface. The radar calibration sphere uses a large number of hexagonal shaped flat membrane panels that are bonded at the perimeter of each panel to form an inflated sphere.<sup>11</sup>

In 1960, NASA launched Echo I, an inflatable sphere satellite bonded together out of a large number of gores of mylar film, 12  $\mu m$  thick, and coated with a 200  $nm$  thick layer of vapor-deposited aluminum. The sphere was 100 feet in diameter, but only weighed 136 pounds and was stowed in a 26 inch diameter spherical container for launch. Echo I was launched to an altitude of 1000 miles to test how inflatable structures worked in space. Unfortunately, the altitude varied over the lifetime of the Echo I experiment due to the effects of solar pressure. Echo I was able to maintain its shape for several months and proved that inflatable structures could work in space.<sup>11</sup>

Sponsorship by the European Space Agency (ESA) drove the development of inflatable structures by Contraves Space Division in Switzerland. Contraves' developmental focus was an axisymmetric reflector antenna for Very Large Baseline Interferometry (VLBI), offset reflectors for mobile communications, and sun shade support structures for telescopes and large sensors. In the early 1980's, a six meter diameter, one-third scale model of a VLBI antenna was built to test the developments made by Contraves. The construction of the antennae was done using two parabolic

membranes, which were supported at the edges by a toroidal structure. The construction utilized the same materials and rigidization techniques that were developed for reflector antenna structures. The support structure intended to use flexible panels, such as Multi-Layer Insulation (MLI) blankets, in each bay, which enables compact mechanical packaging to be achieved below the telescope's structure in a configuration smaller in diameter than the telescope's reflector structure.<sup>11</sup>

## Future

Generally, a payload launched into space uses mechanisms to deploy booms or solar arrays. These mechanisms add mass and therefore cost to the mission. An inflatable structure could reduce the mass and cost by a factor of 100 if it were used to deploy the booms or solar arrays instead of a mechanical mechanism. Future missions envisioned for inflatable structures include inflatable space modules, solar power collectors, and an application of the VBLI in the Advanced Radio Interferometry between Space and Earth (ARISE).

For decades a light-weight durable module has been envisioned to lead the way for further exploration of space. NASA had to abandon its module program, the TransHab project, due to funding problems. Recently, Bigelow Aerospace has picked up where NASA left off on the project. NASA is funding Bigelow Aerospace with a small amount of money but mostly technological expertise from the TransHab Project. The TransHab Project was supposed to be on the ISS, but since it was not, NASA plans to use inflatable modules in the future. The initial launch of one of the modules, seen in Figure 3.4, is envisioned for late 2005. This launch will only test the technology; therefore the module is only one-third scale.<sup>9</sup>



Figure 3.4: Picture of Modules Built By Bigelow Aerospace<sup>9</sup>

The module, named Nautilus, will weigh upwards of 25 tons and offer 330 cubic meters of space. The outer skin will be composed of a synthetic material called Vectran. Vectran has been used on the past three Mars lander missions. It has a strength twice that of other materials such as Kevlar, and performs better at cold

temperatures. In later launches, when the size increased towards full-scale and a person is inhabiting the module, designers envision that the person would deploy water bags with a Velcro backing. The water bags would serve as radiation shielding. A multi-layered, debris-thwarting outer cover protects the inflatable module. A webbing material can be used to divide the interior of the module into compartments, flooring, and other objects that the inhabitant decides is necessary.<sup>9</sup>

In the 1970's, the idea of using a large solar array to collect power and transmit it to Earth, using a microwave beam, was developed. Unfortunately a solar array cluster  $50 \text{ km}^2$  in size orbiting at an altitude of 36,000km would require an antenna in space to have a diameter of one kilometer and the ground based receiving antenna to have a 10 km diameter. The idea of space satellites was abandoned due to the size requirements, but recently the idea has resurfaced. The idea requires changing the orbit altitude to at most 1000km. Inflatable structures are used to expand the solar array once it reaches orbit. Solar array satellites could initially produce power at a rate of 0.1 kilowatts of electricity on the ground per kilogram of mass in orbit. Eventually, the solar collecting array could be expanded to several hundred square kilometers or possibly even thousands of square kilometers.<sup>17</sup>

The Hubble Space Telescope has been circling the Earth for over fourteen years dazzling the public with its pictures of deep space. Unfortunately the mission lifetime of Hubble is coming to an end. One possible replacement is the Advanced Radio Interferometry between Space and Earth (ARISE). As shown in Figure 3.5, ARISE is a giant VLBI mission that consists of one 25m radio telescope in a highly elliptical orbit, which at apogee is a distance of 40,000 km away from the Earth and at perigee is 5,000 km. The antenna will have to be an inflatable structure in order to make this project feasible.<sup>6</sup>

The inflatable antenna can be compacted into a volume 100 times less than a mechanical structure of similar size, and it is five times lighter and six times less expensive to manufacture. The inflation system used to keep the antenna fully expanded is combined with the attitude control and propulsion system to save mass. After launch, when the initial inflation has commenced the structural elements of the ARISE will be rigidized and no more gas will be needed to inflate the structure. The reflector structure has to be kept inflated to get accurate deep-space images, so it will be kept at a pressure of 0.0001 atmospheres. Having a pressure at that level will keep the amount of gas needed to replace the gas that is lost due to micro-meteoroid penetrations.<sup>6</sup>

### 3.2.2 Magnetically Inflated Cable System

Ideas involving inflatable structures are not limited to being inflated by gas. One alternative is called a Magnetically Inflated Cable (MIC). The MIC would take up a small amount of space during launch and are packed into a coil of super-conducting (SC) cables. Once in orbit, the cable would be cryogenically cooled and electrically

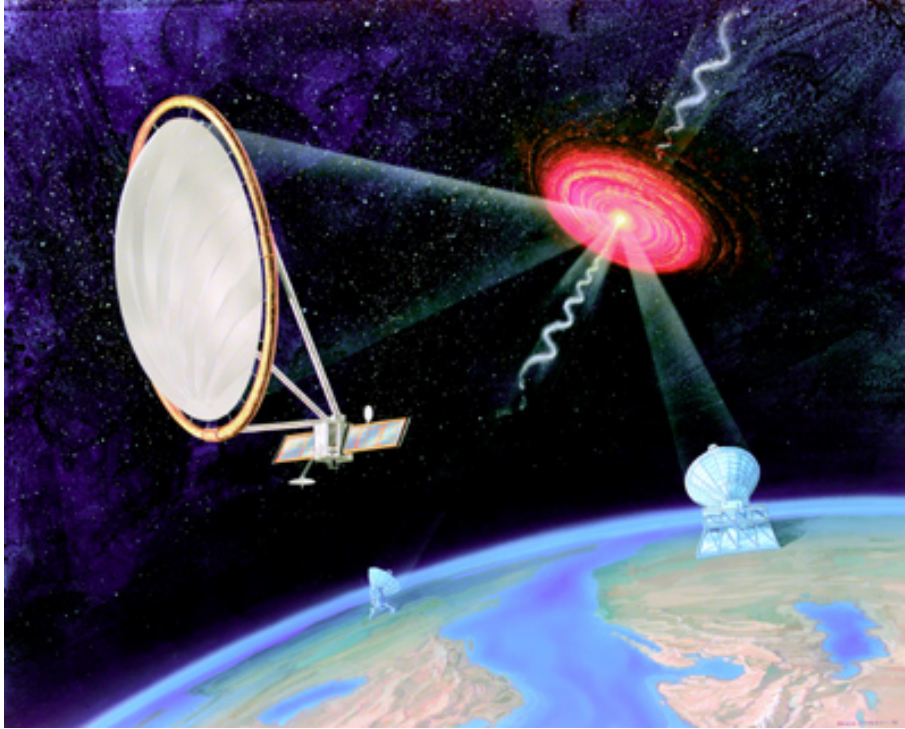


Figure 3.5: ARISE Looking Into Deep Space<sup>6</sup>

charged by a small power supply. The resulting repulsion forces cause the MIC to expand into the final space structure. The SC cables are held firm by a network of high-tensile strength tethers that create a stiff, rigid structure which resist movements in various directions.<sup>22</sup>

The types of SC materials available include  $NbTi$ ,  $Nb_3Sn$ ,  $Nb_3Al$ , YBCO, and BSCCO.  $NbTi$  is the most developed SC and posses desirable attributes such as strength, ductility, stability, and easy fabrication into a variety of forms. The diameter of the filaments is small; on average a micron, which maximizes current density capability and minimizes the effect of local flux jumps on the SC. Recently, ultra-fine filament  $NbTi$  was developed with a diameter on the order of 0.3 microns, which increased the critical current density to  $3 \times 10^6 A/cm^2$ . Despite all of these advantages, there is one major drawback to  $NbTi$ , it is a low temperature SC; the critical temperature required to operate as a SC is below that of helium coolant, 5.6K.<sup>22</sup>

Similarly to  $NbTi$ ,  $Nb_3Sn$  and  $Nb_3Al$  are classified as a low temperature SC (LTS) as well, while YBCO and BSCCO are considered high temperature SC (HTS) with an operating temperature of 70K. Unfortunately, HTS are not as developed as LTS and are much harder to cryostablize than LTS. In light of these drawbacks and the need for further study,  $Nb_3Sn$  appears to be the most promising SC for use as a MIC.  $Nb_3Sn$  operates at 8K and can be fabricated in as fine of filaments as  $NbTi$ .<sup>22</sup>

After selecting a material to compose the SC and constructing the MIC, the MIC

can be used in an application. The MIC applies an electrical charge that causes the SC to expand into the designed structure. Once the structure has achieved the desired shape, permanent beams or supports can be put in place and the MIC can then be charged down.

### 3.2.3 Flying Effector

In the future, space structures are estimated to be much larger than the International Space Station. One problem that has become more apparent with this increased size is the difficulty of constructing such large structures in space without having to risk the lives of astronauts. Previously, the use of robotic arms that could revolve around the station along guiding bars was considered to be the most effective way to build the structure. An example of this can be seen in Figure 3.6 below. In an attempt to eliminate this problem, the University of Tokyo and the National Institute of AIST are teaming together to build a highly effective new space tool referred to as a "flying effector for large space structure assembly." Effectively, this robotic tool can easily move around the spacecraft from point to point without being restrained by a guidance system.<sup>2</sup>

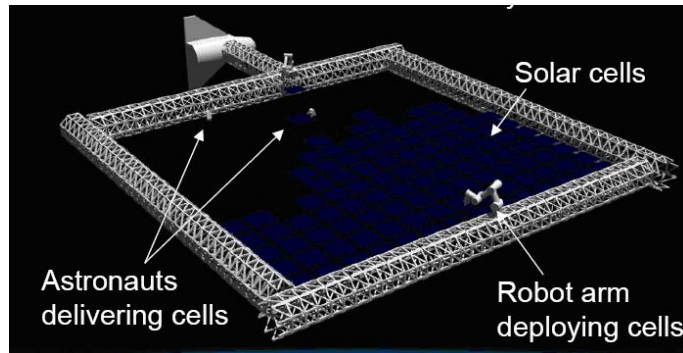


Figure 3.6: Initial Solution to Large Space Construction<sup>2</sup>

Figure 3.7 below is an artistic model of what the robotic construction mechanism may look like. It is estimated to be no more than 20 kg in mass and have a volume around 1024  $in^3$ . It is equipped with cameras, grippers, thrusters, as well as its own tethering system. The effector will work as follows: A command will be sent to the robot informing it of a task. After an analysis of the problem, the robot will recognize the location where it must be to carry out the first step of the procedure. If the spot is across the structure, where a constrained robot could not normally go, it will deploy a tethering device to the location where it needs to be. From there, the effector will ride on the tether to that location and carry out the intended procedure, then move on to the next step.<sup>2</sup>

There are many applications that can be facilitated by the use of an effector. For example, in Figure 3.8, a payload needs to be moved to the other side of the

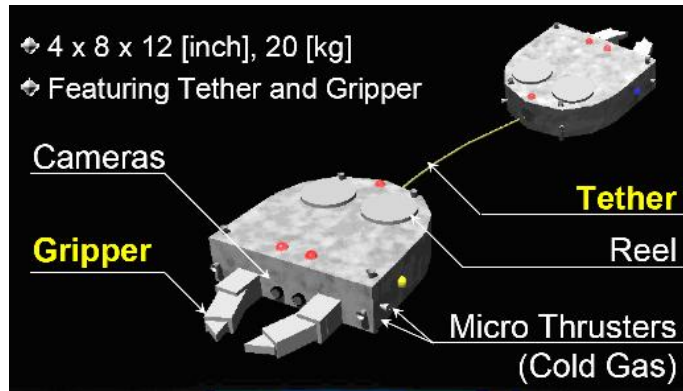


Figure 3.7: More Efficient Solution to Large Space Structure Construction.<sup>2</sup>

large structure. Instead of the robotic arm having to waste a large amount of energy moving around the spacecraft, the effector can deploy across, connect to the other side, tightened its line, and pull the payload across the ship. This greatly reduces the amount of energy losses due to ineffective systems. Another example of the effector application is deploying a membrane across the structure. The effectors grab the membrane from one side of the structure and then tether the membrane to the other side. If the robotic arms were forced to carry out this action, the membrane could possibly be ripped along the way, so the effector also increases reliability in some cases. It must be noted that the effector is not eliminating the use of a robotic arm or astronauts completely; in fact, with all three systems combined, the construction process will be a lot more efficient.<sup>2</sup>

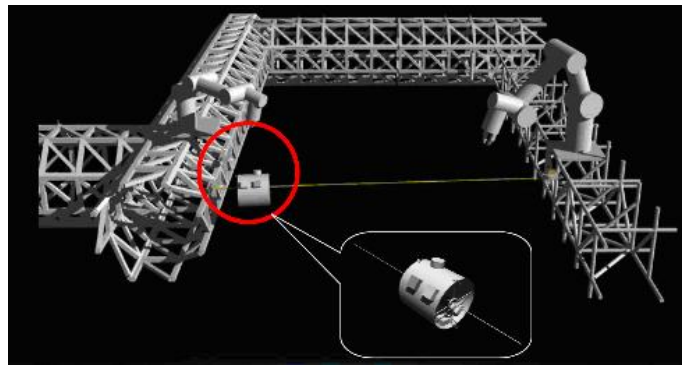


Figure 3.8: Application of Effector Use<sup>2</sup>

### 3.2.4 Nanotubing

In recent years there have been multiple breakthroughs in the material science industry; however, none have been as remarkable as the advances in nanocarbon technol-

ogy. Carbon is a unique fiber because it can form extremely strong bonds with itself; since the bonds form in two dimensional sheets, they can be molded into a multitude different shapes and sizes. Of the structures being created, the most noted are the "ball-shaped" fullerenes and nanotubes, which can be seen below in Figure 3.9. The following presents a summary of the structure, electrical and mechanical properties, and applications of the nanotube technology.<sup>8</sup>

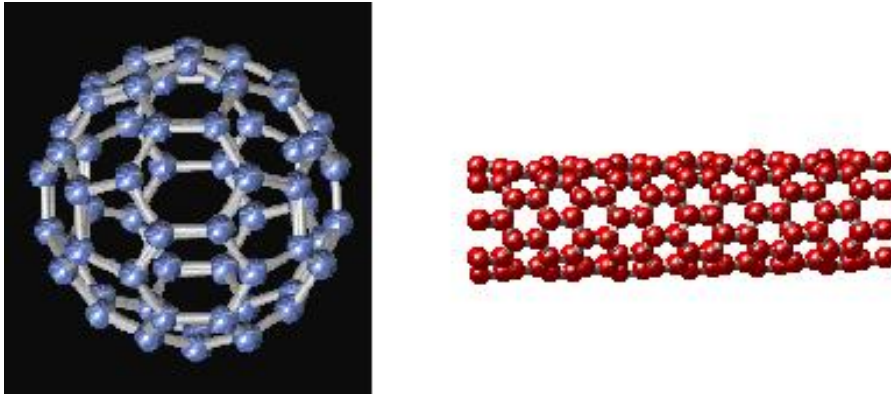


Figure 3.9: Nanotubing<sup>8</sup>

In the future, it is hypothesized that a vast array of materials and products will be produced using nanotubing. Nanotubing is a complex material that is extremely hard to work with; however, through extensive testing in recent years, it has been found to have quite desirable properties. Technically, nanotubes are "cylindrical structures based on the hexagonal lattice of carbon atoms that forms crystalline graphite [PhysicsWeb]." The actual molecule is a matrix of hexagonal carbons atoms that form in sheets which are then rolled into cylindrical structures no more than a nanometer across; this is shown in Figure 3.10. The cylinders can be overlaid or connected in series, but they are always capped with half of a fullerene molecule. This explains why the diameter of the "rope" can be no wider than the diameter of the fullerene molecule.<sup>8</sup>

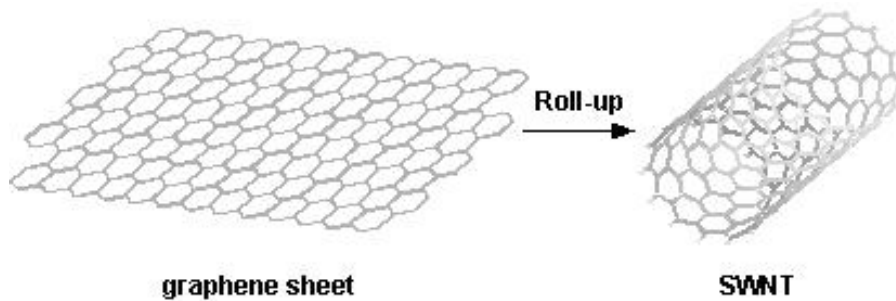


Figure 3.10: Nanotubing Sheet<sup>8</sup>

Armchair, zigzag, and chiral are the three main types of nanotubing. All three depend solely on the method by which the sheet of carbon is rolled. The chiral vector is one of the parameters that determines nanotube type; equation (3.1) displays its mathematical structure.<sup>8</sup>

$$C_h = na_1 + ma_2 \quad (3.1)$$

In equation (3.1),  $n$  and  $m$  are integers while  $a_1$  and  $a_2$  are unit vectors in the two dimensional hexagonal lattice [PhysicsWeb]. As the sheet of nanocarbon molecules are rolled, the ends of the chiral vectors meet; therefore, the magnitude of the vector is equivalent to the circumference of the cylinder. From this, the diameter can subsequently be manipulated by the values picked for  $n$  and  $m$ . A second parameter of nanotubing that determines structure is the angle between the chiral vector,  $C_h$ , and the unit vector  $a_1$ , which can be found using basic matrix algebra. From equation (3.1), if  $n = m$  and the chiral angle is  $30^\circ$ , the structure is typically described as armchar. Zigzag nanotubes are defined by a  $0^\circ$  zero chiral angle and a zero value for either  $n$  or  $m$ ; otherwise, the structure is inherently chiral.<sup>8</sup>

As previously mentioned, nanotubing has many desirable properties that can be very beneficial to engineering purposes. By varying the values of  $n$  and  $m$ , nanotubing can be forced to behave as either a metal or semiconductor. That is, simply by varying the general structure of the molecule, one can achieve two completely different behaviors while maintaining constant chemical composition. One might then envisage nanoscale electronic devices made completely from carbon that would combine the properties of metals and semiconductors, without the need for doping. This material will obviously be revolutionary in industry once we acquire enough information to be able to manipulate the it in an effective way. Another appealing aspect of nanotubing is its strength. It can be over eight times stronger than steel while maintaining a consistency comparable to cellophane or some other light polymer; an actual value of 1 terapascal has even been measured for its Young's modulus. Nanotubes also perform extremely well under compression, unlike other carbon fibers which fracture easily. These mechanical proprieties will have a large affect on the way in which we currently design all types of large structure mechanisms that fatigue under their own weight. With such an easily manipulated structure and the inherited electrical and mechanical properties, it's easy to understand why this could be more than a valuable asset to almost any type of engineering project.<sup>8</sup>

## 3.3 Examples

### 3.3.1 Load and Deflection Nodal Analysis Example

The structure of a spacecraft will have many different sub-structures with different applied loads. An example of the load and deflection analysis of sub-section is shown in Figure 3.11:

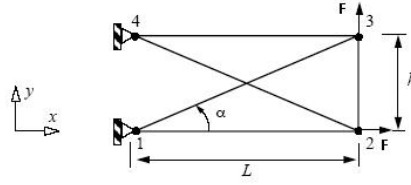


Figure 3.11: Five-bar truss example<sup>20</sup>

The angle  $\alpha$  is  $30^\circ$ , and is related to the length and height by the following equations:

$$\cos \alpha = \frac{L}{\sqrt{L^2 + h^2}} \quad (3.2)$$

$$\sin \alpha = \frac{h}{\sqrt{L^2 + h^2}} \quad (3.3)$$

Forces are applied at the second and third nodes as shown in Figure 3.11, where  $F$  is equal to 100 Newtons and lengths  $h$  and  $L$  are equal to 2 and  $2\sqrt{3}$  meters respectively. The modulus of elasticity is given by  $10 \times 10^9$  Pa, and the areas,  $A$ , of all the bars are equal to  $0.1 \text{ m}^2$ . The restrained structural stiffness matrix is required to relate the loads applied to the structure to the deflections experienced by the structure. The stiffness matrix is defined as part of the unrestrained structural stiffness matrix given by the following equation:

$$[K] = \frac{EA}{L} \begin{bmatrix} \cos^2 \theta & \cos \theta \sin \theta & -\cos^2 \theta & -\cos \theta \sin \theta \\ \cos \theta \sin \theta & \sin^2 \theta & -\cos \theta \sin \theta & -\sin^2 \theta \\ -\cos^2 \theta & -\cos \theta \sin \theta & \cos^2 \theta & \cos \theta \sin \theta \\ -\cos \theta \sin \theta & -\sin^2 \theta & \cos \theta \sin \theta & \sin^2 \theta \end{bmatrix} \quad (3.4)$$

where  $\theta$  is equal to the angle of the bar with respect to the X-axis. The loads applied to the structure are related to the deflections of the structure using the unrestrained structural stiffness matrix in the following equation:

$$\vec{Q} = [K] \vec{q} \quad (3.5)$$

where  $\vec{Q}$  are the loads applied at the specified nodes and  $\vec{q}$  are the corresponding deflections at the same nodes. After the unrestrained structural stiffness matrix is found the restrained structural stiffness matrix may be found by excluding values that aren't at nodes 2 and 3. Therefore, the restrained structural stiffness matrix is derived to be the following:

$$[K_R] = \left( \frac{EA}{L} \right) \begin{bmatrix} 1 + \frac{3\sqrt{3}}{8} & -\left(\frac{3}{8}\right) & 0 & 0 \\ -\left(\frac{3}{8}\right) & \sqrt{3}\left(\frac{9}{8}\right) & 0 & -\sqrt{3} \\ 0 & 0 & 1 + \frac{3\sqrt{3}}{8} & \frac{3}{8} \\ 0 & -\sqrt{3} & \frac{3}{8} & \sqrt{3}\left(\frac{9}{8}\right) \end{bmatrix} \quad (3.6)$$

The deflections at nodes 2 and 3 are found to be:

$$\begin{bmatrix} q_3 \\ q_4 \\ q_5 \\ q_6 \end{bmatrix} = \begin{bmatrix} 0.057 \\ 0.158 \\ -0.038 \\ 0.166 \end{bmatrix} \times 10^{-6} \text{ m} \quad (3.7)$$

### 3.3.2 Material Selection Analysis Example

A particular rod of the structure of a spacecraft must be able to withstand an applied force, but still function properly. This example will compare the properties of aluminum 7075-T6 and AISI 1015 steel to decide which is best for the problem described below. The dimensions of the rod are as follows: volume of  $10 \text{ m}^3$ , cross-sectional area of  $0.1 \text{ m}^2$ , factor of safety of 2, and a  $\sigma_{max}$  of  $150 \text{ MPa}$ . The physical properties of the aluminum 7075-T6 are:  $\sigma_{yield}$  of  $505 \text{ MPa}$  and density,  $\rho$ , equal to  $2810 \text{ kg/m}^3$ ; and the properties of AISI 1015 steel are:  $\sigma_{yield}$  of  $315 \text{ MPa}$  and density,  $\rho$ , equal to  $7870 \text{ kg/m}^3$ . The mass in both cases can be calculated using the following equation:

$$m = \rho \times V \quad (3.8)$$

Therefore the mass of the rod if it were made out of aluminum would be equal to 28,100kg, and the mass of the steel would be equal to 78,700kg. The maximum stress can be calculated using the following equation:

$$\sigma_{max} = \frac{\sigma_y}{FS} \quad (3.9)$$

Therefore, the maximum stress for the aluminum and steel cases are 250 and 158MPa respectively. The maximum force applied may also be calculated by using the following equation:

$$F_{max} = A \times \sigma_{max} \quad (3.10)$$

Therefore, the maximum forces that each part can handle for the aluminum and steel cases are approximately 25N and 16N respectively. Aluminum 7075-T6 is better material because it has a smaller mass and meets all of the other requirements. Steel would not be the best choice because the mass of the rod is minimized as long as the other structural requirements are met.

### 3.3.3 Self Strained Example

The side of a satellite's structure is exposed to the sun is heated by radiation heat transfer; and in order for the structure not to deform due to the compressive forces the caused by the radiation heat transfer the truss, shown in Figure 3.3.3, is designed to prevent deformation. All three bars have the same extensional stiffness  $EA$ , equal to  $10 \times 10^9 \text{ Pa m}^2$ , the length of bar 1-3,L, is  $3m$ , and is heated above the stress free temperature. Bars 1-2 and 2-3 are not heated.

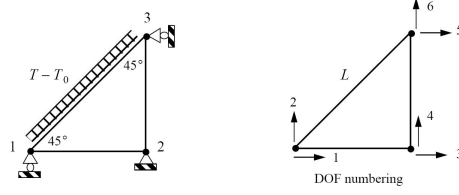


Figure 3.12: Heated structure<sup>20</sup>

The following needs to be found: the fixed-end actions, the unknown nodal displacements, the support reactions and the bar forces.

In order to find the fixed-end actions, nodes 1, 2, and 3 have to be held fixed, or in other words  $q_i = 0$ , and a free body diagram (FBD) drawn, which is shown in Figure 3.13. The mechanical portion of the bar forces vanish for all fixed nodes. Equilibrium at the nodes results in:

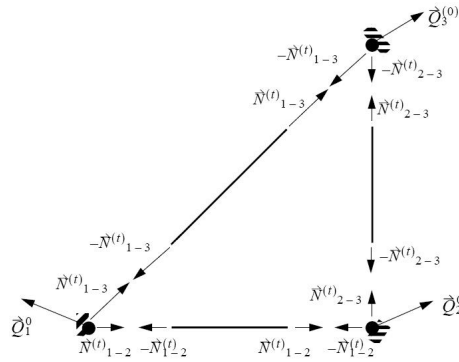


Figure 3.13: FBD of the heated structure<sup>20</sup>

$$\begin{bmatrix} \vec{Q}_1 \\ \vec{Q}_2 \\ \vec{Q}_3 \end{bmatrix}^0 = \begin{bmatrix} -\vec{N}_{1-2}^{(t)} - \vec{N}_{1-3}^{(t)} \\ \vec{N}_{1-2}^{(t)} - \vec{N}_{2-3}^{(t)} \\ \vec{N}_{1-3}^{(t)} + \vec{N}_{2-3}^{(t)} \end{bmatrix} \quad (3.11)$$

The thermal part of the bar forces are obtained using the following equation:

$$\vec{N}_{i-j} = \begin{bmatrix} \cos(\theta) \\ \sin(\theta) \end{bmatrix} \left( EA \left( \frac{\Delta L}{L} \right) - EA\alpha(T - T_0) \right) |_{i-j} \quad (3.12)$$

which gives:

$$\vec{N}_{1-2} = \begin{bmatrix} 1 \\ 0 \end{bmatrix} (-(EA\alpha)_{1-2}(0)) \quad (3.13)$$

$$\vec{N}_{2-3} = \begin{bmatrix} 0 \\ 1 \end{bmatrix} (-(EA\alpha)_{2-3}(0)) \quad (3.14)$$

$$\vec{N}_{1-3} = \begin{bmatrix} \frac{1}{\sqrt{2}} \\ \frac{1}{\sqrt{2}} \\ \frac{1}{\sqrt{2}} \end{bmatrix} (-(EA\alpha)_{1-3}(T - T_0)) \quad (3.15)$$

Hence, the fixed end action vector is:

$$\vec{Q}^0 = \begin{bmatrix} \vec{Q}_1 \\ \vec{Q}_2 \\ \vec{Q}_3 \end{bmatrix}^0 = (-EA\alpha(T - T_0)) \begin{bmatrix} \frac{-1}{\sqrt{2}} \\ \frac{-1}{\sqrt{2}} \\ 0 \\ 0 \\ \frac{1}{\sqrt{2}} \\ \frac{1}{\sqrt{2}} \end{bmatrix} \quad (3.16)$$

To find the unknown nodal displacement the following equation is used:

$$\vec{Q} + (-\vec{Q}^0) = [K] \vec{q} \quad (3.17)$$

which gives us:

$$\begin{bmatrix} Q_1 \\ Q_2 \\ Q_3 \\ Q_4 \\ Q_5 \\ Q_6 \end{bmatrix} + \left( -EA\alpha(T - T_0) \begin{bmatrix} \frac{1}{\sqrt{2}} \\ \frac{1}{\sqrt{2}} \\ 0 \\ 0 \\ \frac{-1}{\sqrt{2}} \\ \frac{-1}{\sqrt{2}} \end{bmatrix} \right) = \left( \frac{EA}{L} \right) \begin{bmatrix} \sqrt{2} + \frac{1}{2} & \frac{1}{2} & -\sqrt{2} & 0 & \frac{-1}{2} & \frac{-1}{2} \\ \frac{1}{2} & \frac{1}{2} & 0 & 0 & \frac{-1}{2} & \frac{-1}{2} \\ -\sqrt{2} & 0 & \sqrt{2} & 0 & 0 & 0 \\ 0 & 0 & 0 & \sqrt{2} & 0 & -\sqrt{2} \\ \frac{-1}{2} & \frac{-1}{2} & 0 & 0 & \frac{1}{2} & \frac{1}{2} \\ \frac{-1}{2} & \frac{-1}{2} & 0 & -\sqrt{2} & \frac{1}{2} & \frac{1}{2} + \sqrt{2} \end{bmatrix} \begin{bmatrix} q_1 \\ q_2 \\ q_3 \\ q_4 \\ q_5 \\ q_6 \end{bmatrix} \quad (3.18)$$

The prescribed nodal displacement and the corresponding reactive nodal forces are:

$$\vec{q}_\beta = \begin{bmatrix} q_2 \\ q_3 \\ q_4 \\ q_5 \end{bmatrix} = \begin{bmatrix} 0 \\ 0 \\ 0 \\ 0 \end{bmatrix} \quad (3.19)$$

$$\vec{Q}_\beta = \begin{bmatrix} Q_2 \\ Q_3 \\ Q_4 \\ Q_5 \end{bmatrix} \quad (3.20)$$

The unknown nodal displacements and the corresponding prescribed nodal forces are:

$$\vec{q}_\alpha = \begin{bmatrix} q_1 \\ q_6 \end{bmatrix} \quad (3.21)$$

$$\vec{Q}_\alpha = \begin{bmatrix} Q_1 \\ Q_6 \end{bmatrix} = \begin{bmatrix} 0 \\ 0 \end{bmatrix} \quad (3.22)$$

Then, the governing matrix equation for the restrained truss is:

$$\begin{bmatrix} 0 \\ 0 \end{bmatrix} + \left( -EA\alpha(T - T_0) \begin{bmatrix} \frac{1}{\sqrt{2}} \\ \frac{-1}{\sqrt{2}} \end{bmatrix} \right) = \left( \frac{EA}{L} \right) \begin{bmatrix} \sqrt{2} + \frac{1}{2} & \frac{-1}{2} \\ \frac{-1}{2} & \sqrt{2} + \frac{1}{2} \end{bmatrix} \begin{bmatrix} q_1 \\ q_6 \end{bmatrix} \quad (3.23)$$

Solving for the unknown nodal displacements:

$$\begin{bmatrix} q_1 \\ q_6 \end{bmatrix} = \left( \frac{L}{EA} \right) \frac{1}{2 + \sqrt{2}} \begin{bmatrix} \sqrt{2} + \frac{1}{2} & \frac{-1}{2} \\ \frac{-1}{2} & \sqrt{2} + \frac{1}{2} \end{bmatrix} \left( -EA\alpha(T - T_0) \begin{bmatrix} \frac{1}{\sqrt{2}} \\ \frac{-1}{\sqrt{2}} \end{bmatrix} \right) \quad (3.24)$$

$$\begin{bmatrix} q_1 \\ q_6 \end{bmatrix} = \frac{L\alpha(T - T_0)}{(2 + \sqrt{2})} \begin{bmatrix} -1 \\ 1 \end{bmatrix} \quad (3.25)$$

The support reactions are determined from  $\vec{Q}_\beta + (-\vec{Q}_\beta^0) = [K_{\beta\alpha}] \vec{q}_\alpha$ . The unknown support reactions are associated with degrees of freedom 2,3,4 and 5. The active displacements are associated with degrees of freedom 1 and 6. Therefore, elements of  $[K_{\beta\alpha}]$  are extracted from rows 2,3,4 and 5 and columns 1 and 6, of the unrestrained structural stiffness matrix given in equation (3.26). The matrix equation for the unknown support reactions is:

$$\begin{bmatrix} Q_2 \\ Q_3 \\ Q_4 \\ Q_5 \end{bmatrix} + \left( -EA\alpha(T - T_0) \begin{bmatrix} \frac{1}{\sqrt{2}} \\ 0 \\ 0 \\ \frac{-1}{\sqrt{2}} \end{bmatrix} \right) = \left( \frac{EA}{L} \right) \begin{bmatrix} \frac{1}{2} & \frac{-1}{2} \\ -\sqrt{2} & 0 \\ 0 & -\sqrt{2} \\ \frac{-1}{2} & \frac{1}{2} \end{bmatrix} \begin{bmatrix} q_1 \\ q_6 \end{bmatrix} \quad (3.26)$$

Substituting the solution for the unknown displacements into this equation to get:

$$\begin{bmatrix} Q_2 \\ Q_3 \\ Q_4 \\ Q_5 \end{bmatrix} = \left( \frac{EA}{L} \right) \begin{bmatrix} \frac{1}{2} & \frac{-1}{2} \\ -\sqrt{2} & 0 \\ 0 & -\sqrt{2} \\ \frac{-1}{2} & \frac{1}{2} \end{bmatrix} \frac{L\alpha(T - T_0)}{(2 + \sqrt{2})} \begin{bmatrix} -1 \\ 1 \end{bmatrix} + EA\alpha(T - T_0) \begin{bmatrix} \frac{1}{\sqrt{2}} \\ 0 \\ 0 \\ \frac{-1}{\sqrt{2}} \end{bmatrix} \quad (3.27)$$

$$\begin{bmatrix} Q_2 \\ Q_3 \\ Q_4 \\ Q_5 \end{bmatrix} = EA\alpha(T - T_0) \begin{bmatrix} \frac{\sqrt{2}}{2 + \sqrt{2}} \\ \frac{\sqrt{2}}{2 + \sqrt{2}} \\ -\frac{\sqrt{2}}{2 + \sqrt{2}} \\ \frac{\sqrt{2}}{2 + \sqrt{2}} \end{bmatrix} \quad (3.28)$$



$$N_{1-3} = \left(\frac{EA}{L}\right) \left( \begin{bmatrix} -\frac{1}{\sqrt{2}} & -\frac{1}{\sqrt{2}} & \frac{1}{\sqrt{2}} & \frac{1}{\sqrt{2}} \end{bmatrix} \begin{bmatrix} q_1 \\ 0 \\ 0 \\ q_6 \end{bmatrix} \right) - EA\alpha(T - T_0) = \\ \left(\frac{EA}{L}\right) \begin{bmatrix} -\frac{1}{\sqrt{2}} & -\frac{1}{\sqrt{2}} \end{bmatrix} \begin{bmatrix} q_1 \\ q_6 \end{bmatrix} - EA\alpha(T - T_0) \quad (3.34)$$

Substitute the solution found for the unknown nodal displacement  $q_1$  and  $q_6$  to get:

$$N_{1-3} = \left(\frac{EA}{L}\right) \begin{bmatrix} -\frac{1}{\sqrt{2}} & -\frac{1}{\sqrt{2}} \end{bmatrix} \begin{bmatrix} q_1 \\ q_6 \end{bmatrix} - EA\alpha(T - T_0) \quad (3.35)$$

$$N_{1-3} = -EA\alpha(T - T_0) \left(\frac{2}{2 + \sqrt{2}}\right) \quad (3.36)$$

So bar 1-3 is in compression for  $T - T_0 > 0$ . Equation 3.29 and Equation 3.30 are used to determine, the axial normal force in bar 2-3:

$$N_{2-3} = \left(\frac{EA}{\frac{L}{\sqrt{2}}}\right) \left( \begin{bmatrix} -0 & -1 & 0 & 1 \end{bmatrix} \begin{bmatrix} q_3 \\ q_4 \\ q_5 \\ q_6 \end{bmatrix} \right) - EA\alpha(0) = \\ \left(\frac{EA}{\frac{L}{\sqrt{2}}}\right) \left( \begin{bmatrix} -0 & -1 & 0 & 1 \end{bmatrix} \begin{bmatrix} 0 \\ 0 \\ 0 \\ q_6 \end{bmatrix} \right) - EA\alpha(0) \quad (3.37)$$

Substitute the solution found for the unknown nodal displacement  $q_6$  to get:

$$N_{2-3} = \sqrt{2} \left(\frac{EA}{L}\right) q_6 = \sqrt{2} \left(\frac{EA}{L}\right) \left(\frac{L\alpha(T - T_0)}{2 + \sqrt{2}}\right) = \frac{\sqrt{2}EA\alpha(T - T_0)}{2 + \sqrt{2}} \quad (3.38)$$

So bar 2-3 is in tension for  $T - T_0 > 0$ .

### 3.3.4 Reaction Wheel Example

Consider the reaction wheel assembly in Figure 3.15. This wheel is used in spacecraft for attitude control. The rotor has been carefully machined to have rotational inertia  $J = 2.56 \times 10^{-3} lbs^2 in$ . The viscous damping constant  $C_\theta$  of the bearings has to be determined by indirect experimental measurement. An electric current is inputed into the motor which spins up the rotor to a high speed. The motor is then shut off

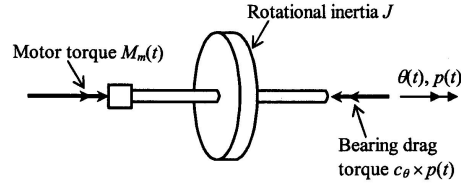


Figure 3.15: Setup diagram for the wheel and the motor<sup>13</sup>

allowing the wheel to spin freely. The spin-down rotational speed is measured with an optical tachometer. At one instant it was found to be  $4000rpm$ , exactly 20.0 seconds later, the measured speed was found to be  $1010rpm$ .

$$J\dot{p} + c_{\theta}p = 0 \quad (3.39)$$

$$\dot{p} + \left(\frac{c_{\theta}}{J}\right)p = 0 \quad (3.40)$$

$$p(t) = Ce^{\frac{c_{\theta}t}{J}} \quad (3.41)$$

$$p(0) = 4000 \times \left(\frac{2\pi}{60}\right) = 418.9rad/s = C \quad (3.42)$$

$$p(20) = 418.9e^{\frac{c_{\theta}20}{(2.56 \times 10^{-3})}} = 1010 \times \left(\frac{2\pi}{60}\right) = 105.77rad/s \quad (3.43)$$

Therefore by taking the natural log of both sides it is found that  $C_{\theta} = 1.7617 \times 10^{-4}lb * in * s$ .

### 3.3.5 Space Shuttle Landing Example

Vertical force is absorbed by a spring system in the landing gear when the space shuttle lands. The Figure 3.16 shows a simplified model to study the landing impact of the space shuttle, where  $m$  is the mass and  $k$  is the stiffness of the landing gear. The space shuttle's sinking speed just before touchdown is denoted as  $V$  and  $g$  is the acceleration due to gravity. The instant the tire makes contact with the ground  $t$  is set at  $t = 0$ . The space shuttle's vertical motion is described by  $y(t)$  relative to the position at  $t = 0$ , as seen in Figure 3.16 on the right hand side. Hence the initial conditions are  $y(0) = 0$  and  $\dot{y}(0) = V$ .

The 2<sup>nd</sup> order ODE of motion for  $y(t)$  (in this case the motion is measured relative to the spring-undeformed position, not relative to the static equilibrium position, so it is necessary to include the body weight  $W = mg$ ) needs to be put into the 2<sup>nd</sup> order ODE of motion in standard form.

$$mg - ky = m\ddot{y} \quad (3.44)$$

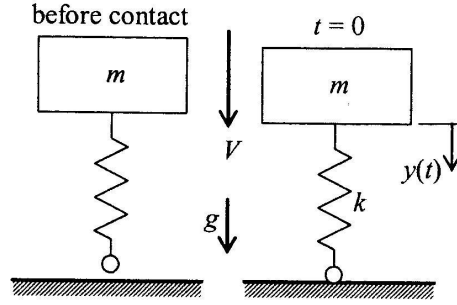


Figure 3.16: Simplified landing gear<sup>13</sup>

By reorganizing the equation the 2<sup>nd</sup> order ODE of motion is rewritten as:

$$\ddot{y} + \left(\frac{k}{m}\right) y = g \quad (3.45)$$

To find the standard form, the right-hand side of the equation is broken up:

$$\ddot{y} + \left(\frac{k}{m}\right) y = \left(\frac{k}{m}\right) \left(\frac{m}{k}\right) g \quad (3.46)$$

which can be rewritten as:

$$\ddot{y} + \omega_n^2 y = \omega_n^2 y(t) \quad (3.47)$$

where:

$$\omega_n = \sqrt{\frac{k}{m}} \quad (3.48)$$

$$y(t) = \frac{gH(t)}{\omega_n^2} \quad (3.49)$$

The initial condition response is:

$$y(t) = \left(\frac{\dot{y}_0}{\omega_n}\right) \sin(\omega_n t) = \left(\frac{V}{\omega_n}\right) \sin(\omega_n t) \quad (3.50)$$

The step response is:

$$y(t) = U(1 - \cos(\omega_n t)) = \left(\frac{g}{\omega_n^2}\right) (1 - \cos(\omega_n t)) \quad (3.51)$$

The total response is:

$$y(t) = \left(\frac{V}{\omega_n}\right) \sin(\omega_n t) + \left(\frac{g}{\omega_n^2}\right) (1 - \cos(\omega_n t)) \quad (3.52)$$

It can be rearranged as follow:

$$y(t) = \frac{g}{\omega_n^2} + \left(\frac{V}{\omega_n}\right) \sin(\omega_n t) - \left(\frac{g}{\omega_n^2}\right) \cos(\omega_n t) \quad (3.53)$$

To express  $\left(\frac{V}{\omega_n}\right) \sin(\omega_n t) - \left(\frac{g}{\omega_n^2}\right) \cos(\omega_n t)$   
in the form of  $C_2(\sin(\omega_n t) \cos(C_3) - \cos(\omega_n t) \sin(C_3))$ :

$$C_2 \cos(C_3) = \frac{V}{\omega_n} \quad (3.54)$$

$$C_2 \sin(C_3) = \frac{g}{\omega_n^2} \quad (3.55)$$

$$C_2 = \sqrt{\left(\frac{V}{\omega_n}\right)^2 + \left(\frac{g}{\omega_n^2}\right)^2} \quad (3.56)$$

$$C_3 = \tan^{-1} \left( \frac{C_2 \sin(C_3)}{C_2 \cos(C_3)} \right) = \tan^{-1} \left( \frac{g}{V\omega_n} \right) \quad (3.57)$$

Therefore the standardize form of the  $2^{\text{nd}}$  order ODE is:

$$y(t) = \frac{g}{\omega_n^2} + \left( \sqrt{\left(\frac{V}{\omega_n}\right)^2 + \left(\frac{g}{\omega_n^2}\right)^2} \right) \sin \left( \omega_n t - \left( \tan^{-1} \left( \frac{g}{V\omega_n} \right) \right) \right) \quad (3.58)$$

The acceleration can be found from this function. The maximum value of the acceleration is then used to determine the maximum force which in turn gives the maximum stress. The stress allows the material to be chosen and the size of the landing gear strut.

### 3.3.6 Vibrations Example

A Pegasus rocket is used to launch a payload into LEO. The rocket is modeled crudely as a mass-spring system with damping. The system is under damped with mass  $m$ , structural, or spring, stiffness  $k$ , and damping coefficient  $\zeta$ . The equation of motion is:

$$m\ddot{x}(t) + c\dot{x}(t) + kx(t) = F(t) \quad (3.59)$$

which can be rewritten in terms of the damping coefficient as:

$$\ddot{x}(t) + 2\zeta\omega_n\dot{x}(t) + \omega_n x(t) = \omega_n^2 u(t) \quad (3.60)$$

where  $u(t) = f(x(t))/k$  and  $\omega_n = \sqrt{k/m}$ .

The forcing function,  $F(t)$ , is found by analyzing the thrust created by the propulsion system. The general solution for any function  $F(t)$  can be solved for though. A rocket at take off has an initial position,  $x(0) = x_0 = 0$ , and initial velocity,  $\dot{x}(0) = \dot{x}_0 = 0$ . Using Laplace transformation on Equation 3.60, the following equation is formed:<sup>13</sup>

$$s^2X(s) - sx(0) - \dot{x}(0) + 2\zeta\omega_n [sX(s) - x(0)] + \omega_n^2X(s) = \omega_n^2L[u(t)] \quad (3.61)$$

where  $L[u(t)]$  is the Laplace transform of the function  $u(t)$  and  $X(s)$  is the Laplace transform of the function  $x(t)$ . Equation 3.61 is then solved for  $X(s)$ , and then the Laplace transform is inverted to determine the value of  $x(t)$ . This leads to two general equations for the output  $x(t)$ :

$$x(t) = e^{-\zeta\omega_n t} \left[ x_0 \cos \omega_d t + \left( \frac{\dot{x}_0 + \zeta\omega_n x_0}{\omega_d} \right) \sin \omega_d t \right] + \frac{\omega_n^2}{\omega_d} \int_{\tau=0}^{\tau=t} e^{-\zeta\omega_n \tau} \sin \omega_d \tau u(t - \tau) d\tau \quad (3.62)$$

$$x(t) = e^{-\zeta\omega_n t} \left[ x_0 \cos \omega_d t + \left( \frac{\dot{x}_0 + \zeta\omega_n x_0}{\omega_d} \right) \sin \omega_d t \right] + \frac{\omega_n^2}{\omega_d} \int_{\tau=0}^{\tau=t} e^{-\zeta\omega_n(t-\tau)} \sin(\omega_d(t - \tau)) u(\tau) d\tau \quad (3.63)$$

where  $\omega_d = \omega_n \sqrt{1 - \zeta^2}$  and  $\tau$  is used as variable to solve the integration. Placing the initial conditions into Equations 3.62 and 3.63 produces the final results for this problem:

$$x(t) = \frac{\omega_n^2}{\omega_d} \int_{\tau=0}^{\tau=t} e^{-\zeta\omega_n \tau} \sin \omega_d \tau u(t - \tau) d\tau \quad (3.64)$$

$$x(t) = \frac{\omega_n^2}{\omega_d} \int_{\tau=0}^{\tau=t} e^{-\zeta\omega_n(t-\tau)} \sin(\omega_d(t - \tau)) u(\tau) d\tau \quad (3.65)$$

these equations can be differentiated to determine the acceleration due to vibrations. The acceleration gives the forces experienced and from there the stress and strain can be determined. The stress and strain help choose the material needed to withstand the vibrational forces caused by the launch.<sup>13</sup>

## 3.4 Conclusion

New launch vehicles are being developed to make it easier to launch multiple satellites and save money at the same time. Modern mechanisms are able to release components without releasing debris into space. Advanced technologies on the horizon include MIC, nanotubing, flying effectors, and inflatable structures. The examples demonstrate how the materials, size of the components, and structural design would be chosen by finding the forces, stresses and load factors that act on the spacecraft.

# Chapter 4

## Conclusions

The five major topics discussed in this report are structures, vibrations, materials, launch vehicles, and new technologies. The area of structures encompasses the beams, plating, and mechanisms used in building the spacecraft. Forces acting on the spacecraft, both during launch and in orbit, are discussed in the Vibrations section. The materials section includes how to select materials based on the materials' properties and interaction with the environment. In the launch vehicles section, six families of launch vehicles are discussed, as well as the mission properties which must be considered when selecting a launch vehicle. Finally, technologies at the forefront of the aerospace industry are discussed, as well as their influences on each of the other four topics.

### 4.1 Structures

Designing a spacecraft's structure to withstand any loads and environmental conditions is critical in creating a successful space mission. The main purpose of structural design is to protect the payload. The most important structures on the spacecraft protect the payload from any possible damage during orbit or takeoff. Structural mechanisms are used for the deployment of sensors and other payload components. Determining which structures are the most reliable and would perform the space mission most effectively is important. One spacecraft structural design will not be best suited for all space missions because of the requirements of each mission.

One aspect of the S&LV functional division was to determine what types of structures are needed for a structural design. Whether the structures would survive their mission duration is another aspect discussed in this report. The main structures involved in a spacecraft's design are the main beams and plating, which compose the chaise of the spacecraft, and the mechanisms involved in the deployment of sensors and components for the mission.

The materials that the beams and plates are composed of are chosen based on the strength and durability the material has in the given environment. Beams are needed

to support the spacecraft during launch and deployment when large forces are applied to the spacecraft. Plates are used to protect the internal components of the spacecraft and insure survival of the payload in space, and also stiffen the structure to deformations. Finite element analysis is one way to analyze how the structure is affected by loads and environmental conditions. Further research on testing techniques could be conducted to determine what kind of stresses the spacecraft can expect in space. Critical sections, such as bolted and welded areas, could also be further studied to come up with more conclusive structural analysis. Cost analysis research would also be important in selecting what structures would be the most viable. Specific beams and plates could be chosen based on the mission's objectives with this research.

Mechanisms, which allow the spacecraft to perform tasks, are another important structural component for a successful space mission. Examples of the tasks that a mechanism can perform are deploying payloads, extending solar arrays, and extending antennas. Different mechanisms can be used to achieve these tasks based on the shape, size, and task that need to be performed. An important design consideration is to minimize the spacecraft's size. Spacecraft components are compacted in order to meet the size consideration and mechanisms are used to expand the compacted structure. Deciding on a particular mechanism may require further research on analytical structure analysis. Research on testing techniques for mechanisms will help in order to determine how the mechanisms fair under the most extreme conditions that the spacecraft may experience in a mission. Determining which mechanism is best for a specific mission is further complicated by the plethora of mechanisms available. The structural decisions will have to be made based on mission prerogatives and the future cost analysis performed on the components.

Beams, plating, and mechanisms are the components that compose the structure of a spacecraft. Beams support the spacecraft during periods when the spacecraft is subjected to large forces, such as launch and deployment. Plates help to stiffen the structure, and protect the internal components of the spacecraft, as well as the spacecraft itself during launch. Mechanisms allow the spacecraft to perform tasks such as deploying a payload or extending solar arrays. The type of beams, plating, and mechanisms used are dependant upon the specific needs of the mission, including the environment to which the spacecraft will be exposed. Thus the spacecraft's structure is designed.

## 4.2 Vibrations

Vibrations and shocks can have negative effects on the proper operation of equipment contained in a spacecraft's payload. Shocks differ from vibrations in that a shock induces an impulse load on the payload, whereas vibrations cause a lower amplitude load over a longer amount of time. The majority of vibrations experienced by a spacecraft occur during launch, and major shocks typically occur during rocket motor ignitions and shutdowns, and during the separation of stages, fairings and other

separable components. Vibrations experienced during the mission may impact the performance of instruments and sensors, but the shocks and vibrations experienced during launch can cause certain components of the payload to fail, or even cause the material failure of the payload structure.

In order to reduce the vibrations imposed on the payload during launch, or reduce the effects of these vibrations on the payload, the vibrations experienced during the launch must be determined. As a preliminary estimate, the launch system is approximated as having only one degree of freedom. The estimate yielded is not accurate enough to use in designing a spacecraft or launch vehicle, but still helps give an idea of the big picture. For a more precise calculation, the finite-element method produces a more acceptable estimate. Since low frequency modes produce the most significant portion of the stress, only the major modes must be included.

The Launch Vehicle Adapter (LVA) is a structure which connects the launch vehicle to the spacecraft. The LVA absorbs the bulk of the vibrations during launch, but the spacecraft will still experience some amount of vibrations. In order to further reduce the vibrations experienced by the spacecraft during launch, the dynamic launch load may be reduced. In order to reduce the effects of these vibrations, the structure could be stiffened. In reality, it is usually a combination of these that is used, yielding an optimum structural stiffness and an optimum dynamic launch load.

Once the payload is delivered safely into space, the proper performance of a spacecraft's instruments and sensors is vital to the success of its mission. The proper functioning of these instruments and sensors may be decreased due to vibrations experienced during the mission. Some possible sources of vibrations on a spacecraft in space are reaction wheels spinning, solar array drives, and the vibrations caused by other small components with moving parts. Two methods of mitigating the effects of these vibrations have been discussed. The Satellite Ultraquiet Isolation Technology Experiment (SUITE) uses a series of active/passive struts to isolate vibrations such that the vibrations are not experienced by the instruments or sensors. Another method, specifically directed at photography of deep space, would fix the camera to another body, separate from the spacecraft. This body would be able to connect to the spacecraft in order to change position, but would then disconnect while the camera gathers data.

A spacecraft may experience vibrations from many different sources during both the launch and its mission. Several methods of diminishing both the effects of vibrations and vibrations themselves have been discussed. Mitigating the effects of vibrations during launch is essential to the safety of the payload. Mission success may depend upon lessening the effects of vibrations during the mission.

### 4.3 Materials

The choice of materials on a mission can directly lead to the success or failure of the mission. If a material is chosen that cannot withstand the environment of space or

forces experienced during launch and deployment, critical instruments and components could be damaged beyond repair. The discussion of materials includes topics such as: material properties, the failure of materials, and the interactions with various environments.

The material properties of a material cover many different aspects ranging from physical properties to electrical properties to thermal properties. Physical properties such as density, modulus of elasticity, maximum allowable stress, and Poisson's ratio are needed to determine how the material will react under applied forces. Engineering design criteria such as tensile stress and shear stress can be determined using these physical properties. Based on whether these stresses are above or below the allowable maximum stresses, the design team can determine how to alter the physical design of the structure.

The effects of temperature on the spacecraft's structure is another important aspect to analyze when determining the best material. Temperature changes in space occur on the order of hundreds of degrees, so choosing a material that does not deform is essential. Thermal properties such as the linear coefficient of thermal expansion and thermal conductivity are available for many materials and allow the design team to determine the heat flux that the structure will undergo, changes in the shape of the structure, and the stresses generated by temperatures on the structure.

When dealing with a spacecraft, other properties such as electrical, optical, and magnetic properties all effect the spacecraft. The resistance and conductivity of the material needs to be known in order to design the electronics of the spacecraft to prevent electrical surges and shorts. Determining how a material resists the magnetic field generated by the electronics is crucial to ensure that the material does not pass on any of the electrical field to other parts of the spacecraft that maybe sensitive to electronics. Painting the outer surface of the structure a certain color could prevent harmful radiation form reaching the electronic components.

All the formulas that are available for calculating all of the design criteria are based on the assumption that the material is manufactured perfectly; however, in reality, this assumption is not good. Cracks can form during the manufacturing processes, weakening the material before any loads are applied to it. Given the size of a crack and the type of material, the critical stress at which the crack propagates can be calculated, along with the fracture toughness. If a design team were to take all of these criteria into consideration when designing the spacecraft, along with a factor of safety, the design should be able to withstand any forces it encounters.

## 4.4 Launch Vehicles

All space related missions require a launch vehicle. The proper launch vehicle must be selected for the mission in question. A launch vehicle cannot be selected until the characteristics of the mission are known. Once the characteristics of the mission are known the launch vehicle can be selected. However, the mission must be structured

such that a currently available vehicle can be used. Designing a launch vehicle for each mission would be a cumbersome and expensive task. There are many operational launch vehicles from which a team can choose. Many launch vehicles display similar characteristics. In light of this, it was determined that the five different launch vehicles mentioned in this report are the most eligible candidates for any mission that is created.

To select a launch vehicle a team must find the best candidate for the mission. The launch vehicle must be capable of supporting the payload of the mission. If a launch vehicle is currently not capable of supporting the payload of the mission, then that launch vehicle is simply not chosen for that mission. The fragility of the payload must also be taken into account. If a launch vehicle produces large amounts of vibrations that would damage the payload, mass must be added so that the payload can dampen out these vibrations. When mass is added to a payload, the cost of the mission increases. So, the launch vehicle selected must produce a minimal amount of vibrations that affect the payload. This issue in accompaniment with the payload support issuer must be analyzed so that the best possible vehicle can be selected. The payload must also reach its desired orbit. Thus launch vehicle power capabilities must be taken into account. The launch vehicle that can most efficiently deliver the payload into the desired orbit altitude is selected. Other factors that affect launch vehicle selection include cost, launch location, inclinations available (a function of the location and propulsive capabilities), and frequency of launches. It is optimal to select the launch vehicle that costs the least. The launch location comes into play when the mission's orbit alignment is considered. It is much easier to launch from a location that puts the spacecraft closer to its final desired orbit. The frequency of available launches is considered when multiple missions are planned in a short period of time. Launch vehicles vary in the time it takes to prepare and launch subsequent missions.

The launch vehicle must also interact well with the spacecraft during launch. The launch vehicle must be capable of supporting the payload's dimensions. Payload fairings can vary dramatically between launch vehicles. Some launch vehicles are capable of carrying only small spacecraft for commercial use while others are capable of carrying multiple spacecraft in their specialized fairings. The recent trend of coupling two or more spacecraft together saves money by launching multiple spacecraft in one launch.

It was determined that six major families of launch vehicles would be capable of supporting most missions designed. The families discussed were the Atlas, K1, Delta, Pegasus/Taurus, Ariane, and Zenit family.

The Atlas family includes the IAS, IIA, IIIB, and the V series. The Atlas launch vehicles are American based, and are launched from either Cape Canaveral, FL or Vandenberg Air Force Base. Most missions that the Atlas vehicles launch are bound for GTO or GEO. The Atlas family allows for a variety of mass capabilities ranging from around 1500 kg to nearly 9,000 kg.

The K1 stands alone as the only launch vehicle in its family. The K1 launch vehicle is used for smaller mass LEO missions. This makes it a prime candidate for commercial missions. The K1 can launch from either Australia or Nevada.

The Delta family is another American based launch vehicle family. Its iterations are the Delta II, IV medium, and the IV heavy. The Delta launch vehicles are capable of sending a range of payload masses from around 2,000 kg to 13,000 kg into either GPS, LEO or even into deep space. Its capabilities make this launch vehicle family very durable. It can be a candidate for nearly any mission.

The Pegasus launch vehicle is primarily used for small mass LEO commercial flights. It is launched from an aircraft, which takes off from an aircraft carrier; therefore Pegasus can achieve a much wider range of inclination angles. Although the Pegasus is not very powerful, it is a prime candidate for small commercial missions in that it can be launched for a cheap price at a variety of inclination angles. In the same family as the Pegasus is the Taurus. The SSLV Taurus, Commercial Taurus, and Taurus XL are American based launch vehicles. Taurus is capable of handling smaller payloads of about 500 kg. It can take its payload into either GTO or LEO from either Vandenberg AFB, or Cape Canaveral. This launch vehicle is great candidate for small missions that desire the higher GTO orbit.

The Ariane family is a newer European Space Agency designed group of launch vehicles. It comes in either the 5G or 5ECA model. The family is capable of launching medium to heavy mass (5000 - 13000 kg) into GTO from Guiana Space Center in South America. The usefulness of the Ariane family comes from its ability to carrying a variety of different sized payload fairings. The launch vehicle was designed with the intent of use for multiple spacecraft launches. If multiple spacecraft are needed for a mission the Ariane deserves the attention and analysis of the team in charge of the mission in question.

The Zenit family of launch vehicles are originally Russian. Zenits come in either the 2SLB land locked Russian vehicle, 3SL, or the 3SLB. The Zenit family is capable of launching medium mass ( 5000 kg) payloads into either LEO or GTO. Recently Boeing got involved with Zenit. This spawned the 3SL, and 3SLB models of the launch vehicle. The usefulness of the Zenit comes from its ability to be launched nearly anywhere in the world. The 2SLB model can only be launched from Baikenur, Russian. The 3SL and 3SLB models can be launched from Baikenur as well. However, a mobile sea platform can be used to launch these models as well. The mobility of the platform allows for nearly any inclination angle. Versatility would be the motivation for the selection of the Zenit family.

The launch vehicles falling into six families of launch vehicles - the Atlas, K1, Delta, Pegasus/Taurus, Ariane, and Zenit families - should facilitate the majority of missions. When selecting a particular launch vehicle several characteristics must be considered. The mission characteristics include mass and size of the payload, desired orbit (both orbit altitude and orbit inclination angle), and frequency of launches needed. These must then be compared with Launch Vehicle Characteristics such as

launch location, power, and cost. Selecting a Launch Vehicle should be the capstone of any space mission.

## 4.5 New Technologies

As our society grows in its technological prowess, new discoveries and conceptions will emerge that help space missions to become safer, more efficient, and more reliable. Three technologies in the near future are discussed in this report. The flying effector will improve the safety of astronauts working in space, while more effectively navigating large structures and increasing the quality of space-built structures. Inflatable structures, if used to replace structural mechanisms, may reduce the mass of a spacecraft, and therefore the cost of launching it into orbit. Nanocarbon, although complex and difficult to manage, can be up to eight times as strong as steel.

Many advances in technology have taken place over the past several years, but nanocarbon technology is theorized to be revolutionary. Carbon is a remarkable element due to its ability to form bonds with itself, with the bonds being two dimensional sheets that vary in shape and size. The most noted shape is the hemisphere tipped nanotube which is a matrix of hexagonal carbon atoms that are in sheets and then rolled into cylinders no longer than a nanometer across. Nanotubing is eight times stronger than steel and works well under compression. There are three types of nanotubing that depend solely on the method which the carbon sheet is rolled; the three types are described by the equation:

$$C_h = na_1 + ma_2 \quad (4.1)$$

where  $n$  and  $m$  are integers,  $a_1$  and  $a_2$  are unit vectors, and  $C_h$  is the angle between the chiral vectors. The first type of nanotubing is called armchair and occurs when  $n = m$  and the chiral angle is thirty degrees. Next, the zigzag occurs when  $n$  or  $m = 0$ , as well as the chiral angle. Finally, if neither an armchair or zigzag is formed then the nanotubing is inherently called chiral. As the nanocarbon is rolled, the chiral vector ends meet and cause the magnitude of the vector to equal the circumference of the cylinder, which is true for all three types of nanotubing. In the future, there are going to be extreme advances in regards to creating materials and products using nanotubing. Now, however, there is not enough knowledge to complete such a task since nanotubing proves to be complex and hard to manage.

The concept of an inflatable structure is hardly new. Goodyear developed the idea during the 1950's, and NASA was quick to implement the idea into space missions, as evidenced by their 1960 launch of Echo I. Echo I was an inflatable sphere satellite. Echo I demonstrated the use of inflatable structures in space on a large scale. On a smaller scale, inflatable structures could replace mechanisms used to deploy structural components such as antennae or solar arrays. This would greatly reduce the mass of the spacecraft, thereby reducing the cost of the mission.

Space structures in the future have been proposed to be larger than the current International Space Station. Although a larger size seems to produce only positive aspects, in truth, it is arduous to construct large structures in space without endangering the safety of astronauts. Currently, the most effective way to build a structure in space is through the use of robotic arms; however, there is a novel idea that will facilitate these robots' work load. It is called the: "flying effector for large space structure assembly." This structure will allow a robotic devices, called the effector, to move from point to point without a grounded guidance system. The effector is intended to have a mass of twenty kilograms and a volume of 1024 cubic inches. It will be equipped with cameras, grippers, thrusters, and its own personal tethering system. The effector will evaluate received commands and calculate the most efficient way to perform a job. Finally, the effector carries out the intended procedure and then moves onto the next. The effector is not intended to completely nullify the use of the robotic arm and the need for astronauts, but in turn, hopes to work hand in hand with the two to ensure better quality, and a more effective way to navigate around large structured spacecraft.

Nanocarbon, inflatable structures, and the flying effector are technologies and concepts on the forefront of the space industry. When implemented into space missions, they may improve safety, efficiency, and reliability. However, these are only three examples. In the future, many more developments will work together to improve space missions.

## 4.6 Summary

Comprising the study of Spacecraft Structures and Launch Vehicles are five major topics: Structures, Vibrations, Materials, Launch Vehicles, and New Technologies. New Technologies will improve all areas of space mission engineering. The structure of a spacecraft enables the spacecraft to survive both the launch and the environment of space while performing its mission. Vibrations affect the structure as well as the operation of equipment contained on the spacecraft. A launch vehicle must be selected by matching payload characteristics and desired mission characteristics with properties of the launch vehicle. When tied together in a single package these topics comprise an important part in the planning and designing a space mission.

# Bibliography

- [1] *Thin-Walled Pressure Vessels*. efunda.com, Sunnyvale, California, 2003.
- [2] Tatsuya Arai, Toshiaki Iwata, and Machida Mazuo. *Flying Effector To Support Large Space Structure Construction*. University of Toyko, Toyko, Japan, 2004.
- [3] Ferdinand Beer and et al. *Spacecraft Materials Requirements and Applications*. McGraw-Hill Companies, Inc., New York, New York, 1993.
- [4] Ferdinand Beer and et al. *Mechanics of Materials*. McGraw-Hill Companies, Inc., New York, New York, 2002.
- [5] William Callister Jr. *Materials Science and Engineering, an Introduction, 6th Edition*. John Wiley & Sons, Inc., Ontario, Canada, 2003.
- [6] Art B Chmielewski and et al. *ARISE Mission and Spacecraft Description*. Jet Propulsion Laboratory, Pasadena, California, 1998.
- [7] Starsys Corporation. *Quknut 3k Product Information*. Starsys Corporation, Boulder, Colorado, 2004.
- [8] Vincent H. Crespi. *NANOTUBES & BUCKYBALLS*. Penn State, State College, Pennsylvania, 2004.
- [9] Leonard David. *Inflatable Space Outposts: Cash Down on High Hopes*. Space.com, Las Veags, Nevada, 2001.
- [10] Keith K. Denoyer and Conor D. Johnson. *Recent Achievements in Vibration Isolation Systems for Space Launch and On-Orbit Applications*. CSA Engineering, Mountain View, California, 2001.
- [11] R. E. Freeland, G. D. Bilyeu, G. R. Veal, and M. M. Mikulas. *Inflatable Deployable Space Structures Technology Summary*. IAF, Tustin, California, 2001.
- [12] Mark S. Grahne and David P. Cadogan. *Inflatable Solar Arrays: Revolutionary Technology* Society of Automotive Engineers., Frederica, Delaware, 1998.

- [13] W. H. Hallauer. *Vehicle Vibrations & Controls*. Virginia Tech, Blacksburg, Virginia, 2004.
- [14] Wade Henning, Justin Bowen, and Sean Dougherty. *Emerald Inter-Satellite Separation System*. AFRL Nanosat Committee, Stanford, California, 1999.
- [15] Steven J. Isakwitz, Joshua B. Hopkins, and Joseph P. Hopkins Jr. *International Reference Guide to Space Launch Systems (4th Edition)*. AIAA, Reston, Virginia, 2004.
- [16] Zelina Iskanderova and Jacob I. Kleiman. *Protection of Materials and Structures from Space Environment*. Kluwer Academic, 3300 AZ Dordrecht, The Netherlands, 2003.
- [17] Michael T. Izumi. *Mechanisms for Reliable One-Time Deployment of Panels*. Goddard Space Flight Center, Greenbelt, Maryland, 2002.
- [18] Conor D. Johnson and Paul S. Wilke. *Whole-Spacecraft Shock Isolation System*. CSA Engineering, Mountain View, California, 2000.
- [19] Eric R. Johnson. *Thin Walled Structures, AOE 3024*. University Printing Services, Blacksburg, Virginia, 2003.
- [20] Eric R. Johnson. *Homework 8 for AOE 3124*. A-1 Copies, Blacksburg, Virginia, 2004.
- [21] W. J. Larson and J. R. Wertz. *Space Mission Analysis and Design*. McGraw-Hill Companies, Inc., New York, New York, 2004.
- [22] James Powell, George Maise, and John Paniagua. *MIC - A Self Deploying Magnetically Inflated Cable System for Large Scale Space Structures*. Plus Ultra Technologies, Inc., Shoreham, New York, 2000.
- [23] Thomas P. Sarafin. *Spacecraft Structures and Mechanisms*. Kluwer Academic, 1995.